Benthic Foraminiferal response to sea level change in the mixed siliciclastic-carbonate system of southern Ashmore Trough (Gulf of Papua)

Brooke E. Carson,[1,2] Jason M. Francis,[1,2] R. Mark Leckie,[3] André W. Droxler,[1] Gerald R. Dickens,[1] Stéphan J. Jorry,[1,4] Sam J. Bentley,[5] Larry C. Peterson,[6] and Bradley N. Opdyke[7]

[1] Ashmore Trough in the western Gulf of Papua (GoP) represents an outstanding modern example of a tropical mixed siliciclastic-carbonate depositional system where significant masses of both river-borne silicates and bank-derived neritic carbonates accumulate. In this study, we examine how benthic foraminiferal populations within Ashmore Trough vary in response to sea level–driven paleoenvironmental changes, particularly organic matter and sediment supply. Two 11.3-m-long piston cores and a trigger core were collected from the slope of Ashmore Trough and dated using radiocarbon and oxygen isotope measurements of planktic foraminifera. Relative abundances, principal component analyses, and cluster analyses of benthic foraminiferal assemblages in sediment samples identify three distinct assemblages whose proportions changed over time. Assemblage 1, with high abundances of *Uvigerina peregrina* and *Bolivina robusta*, dominated between ~83 and 70 ka (early regression); assemblage 2, with high abundances of *Globocassidulina subglobosa*, dominated between ~70 and 11 ka (late regression through lowstand and early transgression); and assemblage 3, with high abundances of neritic benthic species such as *Planorbulina mediterranensis*, dominated from ~11 ka to the present (late transgression through early highstand). Assemblage 1 represents heightened organic carbon flux or lowered bottom water oxygen concentration, and corresponds to a time of maximum siliciclastic fluxes to the slope with falling sea level. Assemblage 2 reflects lowered organic carbon flux or elevated bottom water oxygen concentration, and corresponds to an interval of lowered siliciclastic fluxes to the slope due to sediment bypass during sea level lowstand. Assemblage 3 signals increased off-shelf delivery of neritic carbonates, likely when carbonate productivity on the outer shelf (Great Barrier Reef) increased significantly when it was reflooded. Benthic foraminiferal assemblages in the sediment sink (slopes of Ashmore Trough) likely respond to the amount and type of sediment supplied from the proximal source (outer GoP shelf).

1. Introduction

[2] The greater Gulf of Papua (GoP) region (Figure 1) extends over ~100,000 km^2 between southern Papua New Guinea (PNG), northeast Australia and the Coral Sea. The region has been selected as one of two focus areas for the MARGINS Source-to-Sink (S2S) Initiative because of its semienclosed nature, low-latitude location, relatively undisturbed environment, and significant siliciclastic and carbonate sediment sources [*National Science Foundation*, 2003]. Several major rivers, most notably the Fly, drain into the GoP on the northwest coast, delivering some 200 to 300 megatonnes per year of siliciclastic sediment to the inner shelf [*Harris et al.*, 1993; *Milliman*, 1995]. At present day, currents preferentially transport this fluvially derived sediment along the shelf in a clockwise manner [*Wolanski and Alongi*, 1995; *Wolanski et al.*, 1995], leaving much of the middle and outer GoP shelf southwest of the Fly River devoid of Holocene siliciclastic sediment [*Harris et al.*, 1996]. In the southwest GoP, the Great Barrier Reef (GBR)

---

[1]Department of Earth Science, Rice University, Houston, Texas, USA.
[2]Now at Chevron Energy Technology Company, Houston, Texas, USA.
[3]Department of Geosciences, University of Massachusetts, Amherst, Massachusetts, USA.
[4]Division Etudes and Conseils, Beicip-Franlab, Rueil-Malmaison, France.
[5]Earth Sciences Department, Memorial University of Newfoundland, St. John's, Newfoundland & Labrador, Canada.
[6]Rosenstiel School of Marine and Atmospheric Science, University of Miami, Miami, Florida, USA.
[7]Department of Earth and Marine Science, Australian National University, Canberra, ACT, Australia.
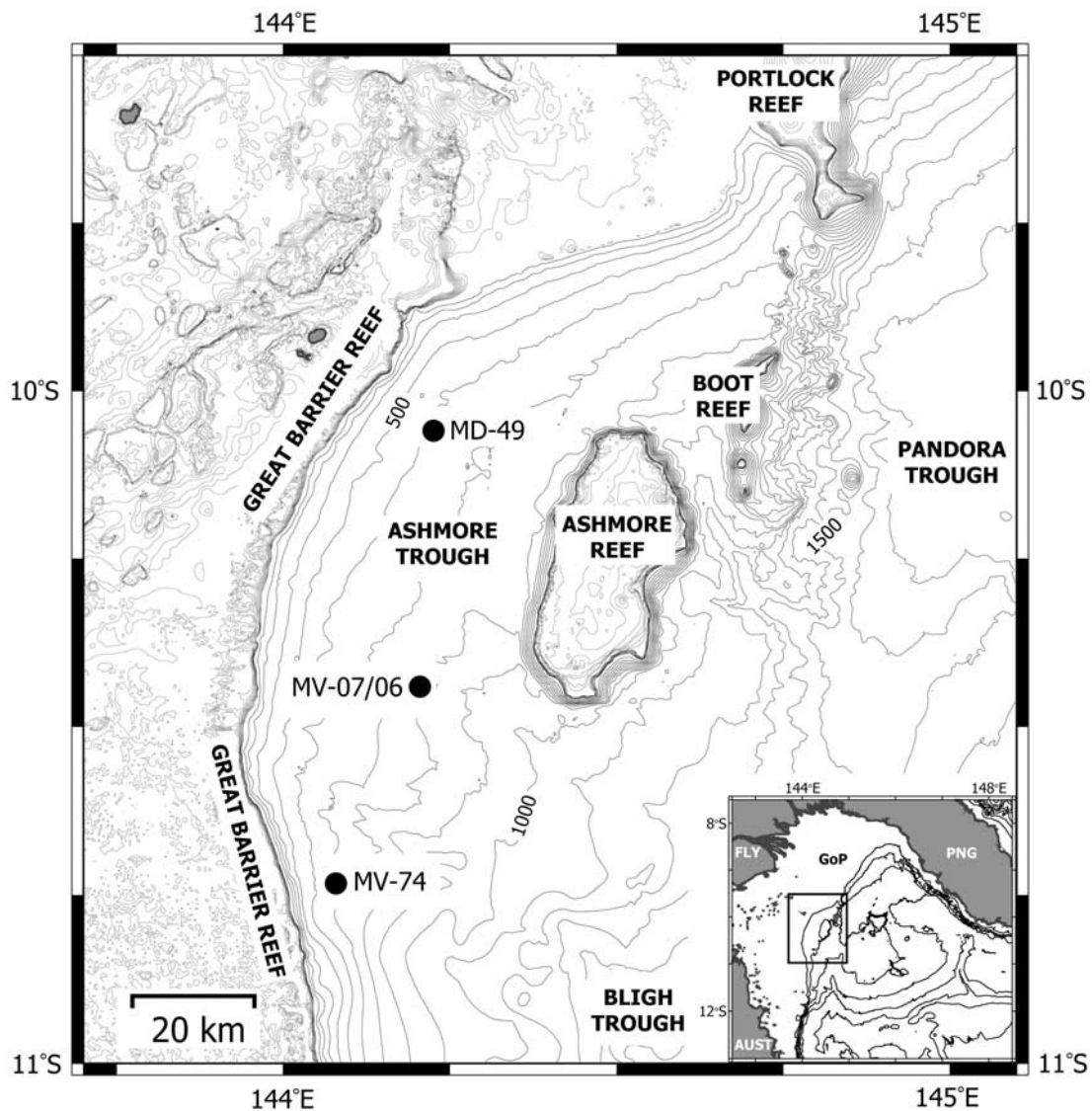
**Figure 1.** Bathymetric map of the Gulf of Papua showing the location of the two cores used in this study, MV-74 and MV-07/06, as well as Core MD05-2949 (MD-49) used in chronostratigraphic control of cores MV-74 and MV-07/06. Abbreviations used are GoP (Gulf of Papua), PNG (Papua New Guinea), Aust (Australia), and Fly (Fly River). Contours are 500 m on regional inset map of GoP. Figure is from *Francis et al.* [2006].

on the middle to outer shelf and several atoll systems on isolated offshore platforms produce substantial amounts of carbonate material [e.g., *Harris et al.*, 1993; *Jorrey et al.*, 2008; *Francis et al.*, 2006]. Both siliciclastic and neritic carbonate sediments escape the shelf and platforms to adjacent slopes and basins of the GoP, although at different rates depending on location [*Brunskill et al.*, 1995; *Walsh and Nittrouer*, 2003; *Jorry et al.*, 2008]. Crucially, the amounts and types of sediment reaching the slope have varied significantly over time in response to environmental changes, particularly sea level [*Jorry et al.*, 2008; *Francis et al.*, 2006].

[3] A primary goal of the MARGINS S2S NSF program is to quantify how variations in sediment production, transport, and accumulation are preserved in the stratigraphic record [*National Science Foundation*, 2003]. Fossils of

foraminifera are important components of the stratigraphic record, being widely utilized to reconstruct paleoenvironmental conditions, including water depth, temperature, salinity, dissolved oxygen, and organic carbon supply [e.g., *Murray*, 1991; *Sen Gupta*, 1999a; *Culver and Buzas*, 2000]. Along continental margins, changes in sea level can greatly alter environmental conditions at the seafloor and in the water column, significantly influencing foraminiferal communities [e.g., *Murray*, 1991; *Leckie and Olson*, 2003, and references therein]. However, few studies have examined foraminiferal communities along the slopes of tropical mixed siliciclastic-carbonate margins, common depositional environments both today and in the past. Evaluating sediment accumulation, including foraminiferal assemblages, in recent sediments (e.g., late Pleistocene to Holocene) where the timing and magnitude of sea level change are relatively
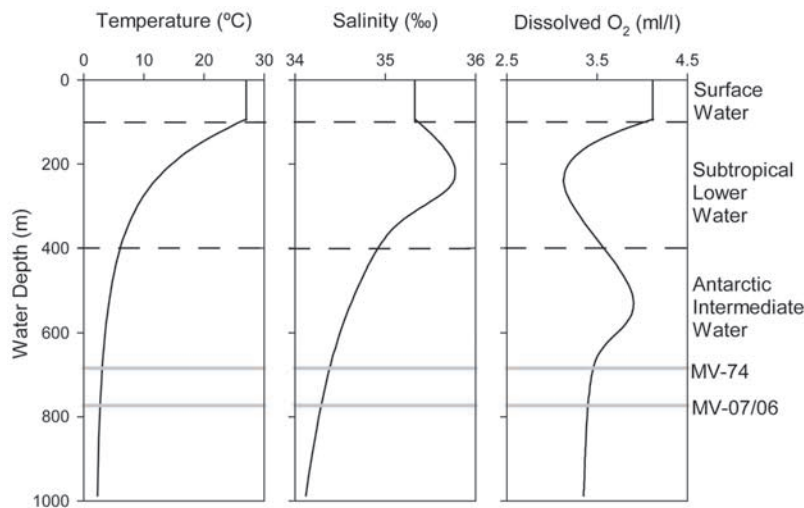
Figure 2. Schematic representation of temperature, salinity, and dissolved oxygen profiles in the Gulf of Papua shown with modern water masses, after *Wyrtki* [1962], *Pickard et al.* [1977], and *Wolanski et al.* [1995]. MV-74 and MV-07/06 are indicated at their modern water depths.

well constrained and high-resolution chronostratigraphy can be established using a combination of absolute dating techniques [e.g., *Chappell*, 2002; *Lambeck et al.*, 2002] is critical for interpreting ancient mixed depositional settings.

[4] Ashmore Trough in the western GoP (Figure 1) represents an outstanding modern example of a tropical mixed siliciclastic-carbonate system. Recent studies demonstrate that siliciclastic and carbonate fluxes to Ashmore Trough varied considerably during the late Quaternary in response to sea level [*Francis et al.*, 2006]. Consequently, this area provides an intriguing location to test the sensitivity of the benthic foraminiferal assemblages to paleoenvironmental changes in a poorly studied but relatively common depositional setting. In this work, we examine benthic foraminiferal assemblages in two well-dated sediment cores from slopes of Ashmore Trough. Additionally, we determine sedimentary fluxes of organic carbon, typically a limiting factor for benthic organisms living in the deep ocean [e.g., *Gooday*, 1988; *Jorissen et al.*, 1995; *Thomas and Gooday*, 1996; *Schmiedl et al.*, 1997; *Jorissen*, 1999; *Kaiho*, 1999; *Loubere and Fariduddin*, 1999]. These results provide better understanding of late Pleistocene to Holocene sediment accumulation and paleoenvironmental change in Ashmore Trough. Here we demonstrate that benthic foraminiferal assemblages provide an important proxy record of sea level-forced changes in sediment and organic carbon fluxes. Our results complement earlier studies of foraminiferal response to organic matter availability and additionally, provide the added dimension of fluctuating inputs of siliciclastic and carbonate platform sediments as sea level fell and subsequently rose during the last glacioeustatic cycle.

2. Study Area and Oceanographic Setting

2.1. Ashmore Trough

[5] Ashmore Trough is the smallest and westernmost basin in the GoP, representing an upper slope environment with maximum depths of ∼800 m (Figure 1). The PNG continental shelf lies to the north, where the shelf-slope break varies between ∼110 and 130 m. Ashmore Trough is bounded by extensive reef systems of the GBR to the west and Ashmore and Boot Atolls to the east. The barrier along the GBR and the rims of the offshore atolls have aggraded almost to sea level, whereas the depths of the surrounding shelf and lagoons average 50-60 m. The little amount of siliciclastic sediment (10 to 20% [*Muhammad et al.*, 2008]) presently entering Ashmore Trough through the water column probably comes from the north, while neritic carbonates are sourced from the reef systems to the west and east.

2.2. Modern Oceanography

[6] Surface waters of the GoP lie within the latitudinal band of tropical waters characterized by relatively high temperatures of 25°–29°C. The surface waters of the outer shelf and GoP basin are generally well mixed to a depth of ∼100 m and typically express normal marine salinities of ∼34.5–35.5‰ (Figure 2) [*Pickard et al.*, 1977; *Wolanski et al.*, 1995]. These waters are predominately brought into the GoP by the westward flowing South Equatorial Current (SEC), producing overall convergence in the region [*Wyrtki*, 1960; *Pickard et al.*, 1977]. Surface circulation in the GoP is dominated by a clockwise gyre generated under the influence the Coral Sea Coastal Current [*Wolanski et al.*, 1995].

[7] Two subsurface water masses are recognized in the GoP, Subtropical Lower Water (SLW) and Antarctic Intermediate Water (AAIW). SLW has a core depth between 100 and 250 m and contains maximum salinities (∼35.5–36.0‰) and minimum dissolved oxygen concentrations (∼3.0 mL/L) [*Wyrtki*, 1962; *Pickard et al.*, 1977; *Wolanski et al.*, 1995]. Below SLW, there is a transitional zone and AAIW, which forms the "bottom" water in the region. AAIW has a core depth of ∼650 to 1150 m and contains minimum salinities (∼34.4–34.5‰) and maximum dissolved oxygen concentrations (∼4.0 mL/L) [*Wyrtki*, 1962; *Pickard et al.*, 1977; *Wolanski et al.*, 1995].

2.3. Sea Level Change and Past Sediment Fluxes

[8] The last glacial cycle (∼130 ka to the present) was a time of large climate fluctuations and high-amplitude eu-
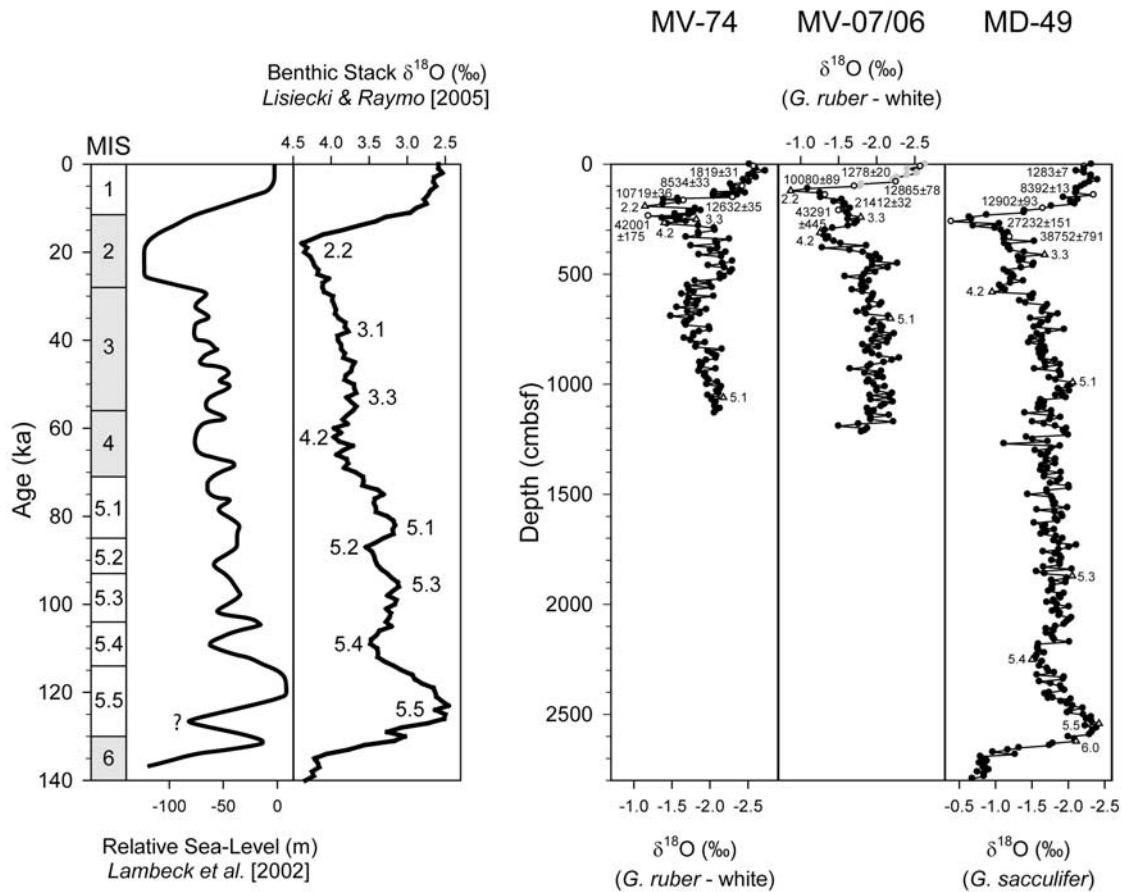
Figure 3. Eustatic sea level curve for the last glacial cycle [*Lambeck et al.*, 2002], the stacked record of benthic foraminifera oxygen isotopes [*Lisiecki and Raymo*, 2005], and the *Globigerinoides ruber* oxygen isotope records from Ashmore Trough (this study). The chronology for MV-74 and MV-07/06 is based on correlation with oxygen isotope excursions (open triangles) and calibrated radiocarbon ages (open circles). Additional chronostratigraphic control, including the ages of the base of MV-74 and MV-07/06, is provided by comparison with the planktic oxygen isotope record of a 36.5 m core taken in Ashmore Trough, MD05-2949 (MD-49, shown on far right). Data obtained from MV-06 are indicated in gray.

static sea level changes (Figure 3), which undoubtedly impacted carbonate and siliciclastic deposition in Ashmore Trough. Along margins with tropical reef systems, neritic carbonate fluxes to adjacent slopes are generally highest during late transgressions and highstands [e.g., *Droxler*, 1984; *Droxler and Schlager*, 1985; *Handford and Loucks*, 1993; *Schlager et al.*, 1994]. This is clearly the case along the northeast Australian margin south of the study area [*Dunbar et al.*, 2000; *Page et al.*, 2003], as well as within Ashmore Trough [*Francis et al.*, 2006] and Pandora Trough [*Jorry et al.*, 2008]. Past siliciclastic accumulation on slopes and basins adjacent to tropical reef systems is not so straightforward. Often, it has been suggested that siliciclastic accumulation is highest during lowstands, which may be the case in some locations [*Handford and Loucks*, 1993; *Schlager et al.*, 1994]. However, south of Ashmore Trough and for at least the last glacioeustatic cycle, siliciclastic fluxes to slopes east of the GBR were at a minimum during lowstand and at a maximum during late transgression [*Dunbar et al.*, 2000; *Page et al.*, 2003]. Our work in

Ashmore Trough suggests a somewhat different response: low siliciclastic fluxes during lowstand, highest siliciclastic fluxes during early sea level regression, and high siliciclastic fluxes during late transgression [*Francis et al.*, 2006]. Possible causes for this siliciclastic response to sea level are discussed elsewhere [*Dunbar et al.*, 2000; *Page et al.*, 2003; *Harris et al.*, 2005; *Francis et al.*, 2006] and below.

[9] Following *Lambeck et al.* [2002], we categorize various stages of sea level over the past 130 ka as follows (Figure 3). The interval between ~130 and 115 ka is the last interglacial highstand, when sea level is mostly within 20 m of, or slightly higher than, present day. The interval between ~115 and 71 ka corresponds to early regression, when sea level oscillated between ~20 and 50 m below modern sea level. The interval between ~71 and 30 ka represents late regression, when sea level was between ~50 and 75 m below present day. Eustatic sea level was at lowstand between ~30 and 14 ka, which included the Last Glacial Maximum (LGM, 25–19 ka), when sea level reached ~120 m below present-day levels and never exceeded

Table 1. The $\delta^{18}O$ Values of the Planktic Foraminifer *Globigerinoides ruber* (250- to 300-μm-Size Fraction) and Total Organic Contents and Mass Accumulation Rates for MV-74, MV-06, and MV-07[a]

Table 1. (continued)

Sample Depth, cm	$\delta^{18}O$, ‰	TOC, weight%	TOC MAR, g/cm^{2}ka
MV-74			
0−2	−2.52	0.450	0.056
10−12	−2.58	-	-
20−22	−2.60	0.330	0.048
30−32	−2.73	-	-
40−42	−2.57	0.250	0.038
50−52	−2.51	-	-
60−62	−2.61	0.230	0.035
70−72	−2.44	-	-
80−82	−2.51	0.270	0.042
90−92	−2.27	-	-
100−102	−2.43	0.350	0.090
110−112	−2.30	-	-
120−122	−2.41	0.490	0.099
125−127	−2.06	-	-
130−132	−2.46	0.480	0.097
135−137	−2.05	-	-
140−142	−2.36	0.790	0.184
145−147	−2.05	-	-
150−152	−2.30	0.770	0.053
155−157	−1.58	-	-
160−162	−1.39	0.450	0.035
165−167	−1.66	-	-
170−172	−1.59	0.230	0.009
180−182	−1.39	0.200	0.007
190−192	−1.15	-	-
200−202	−1.81	0.220	0.005
210−212	−1.88	-	-
215−217	−1.73	-	-
220−222	−1.79	0.230	0.005
225−227	−1.54	-	-
230−232	−1.73	-	-
235−237	−1.19	-	-
240−242	−1.61	0.280	0.003
245−247	−1.37	-	-
250−252	−1.82	-	-
255−257	−1.57	-	-
260−262	−1.69	0.380	0.007
265−267	−1.40	-	-
270−272	−1.44	-	-
280−282	−1.85	0.620	0.314
290−292	−2.06	-	-
300−302	−2.07	0.720	0.413
310−312	−1.85	-	-
320−322	−1.85	0.610	0.350
330−332	−1.69	-	-
340−342	−2.26	0.680	0.379
350−352	−2.08	-	-
360−362	−2.10	-	-
370−372	−1.75	-	-
380−382	−2.10	-	-
390−392	−2.01	0.610	0.361
400−402	−2.21	-	-
410−412	−1.86	-	-
420−422	−2.15	-	-
430−432	−	-	-
440−442	−2.30	0.540	0.319
450−452	−2.17	-	-
460−462	−1.98	-	-
470-472	−2.19	-	-
480−482	−2.29	-	-
490−492	−2.27	0.560	0.322
500−502	−2.13	-	-
510−512	−2.19	-	-
520−522	−2.14	-	-
530−532	−1.81	-	-
540−542	−1.99	0.580	0.333
550−552	−1.71	-	-
560−562	−2.03	-	-
570−572	−1.73	-	-
580−582	−1.79	-	-
590−592	−1.63	0.610	0.350
600−602	−2.05	-	-
610−612	−1.72	-	-
620−622	−1.85	-	-
630−632	−1.70	-	-
640−642	−1.82	0.510	0.300
650−652	−1.57	-	-
660−662	−1.96	-	-
670−672	−1.71	-	-
680−682	−1.87	-	-
690−692	−1.49	0.550	0.320
700−702	−1.76	-	-
710−712	−1.72	-	-
720−722	−1.67	-	-
730−732	−1.69	-	-
740−742	−1.99	0.510	0.293
750−752	−2.00	-	-
760−762	−1.86	-	-
770−772	−1.79	-	-
780−782	−1.79	-	-
790−792	−1.66	0.450	0.270
800−802	−1.75	-	-
810−812	−1.94	-	-
820−822	−1.83	-	-
830−832	−1.82	-	-
840−842	−2.16	0.560	0.343
850-852	−1.98	-	-
860−862	−2.03	-	-
870−872	−2.09	-	-
880−882	−2.08	-	-
890−892	−1.95	0.380	0.240
900−902	−1.87	-	-
910−912	−1.90	-	-
920−922	−1.88	-	-
930−932	−2.08	-	-
940−942	−1.86	0.290	0.189
950−952	−1.94	-	-
960−962	−1.93	-	-
970−972	−1.96	-	-
980−982	−1.99	-	−
990−992	−2.10	0.260	0.171
1000-1002	−1.96	-	-
1010−1012	−2.15	-	-
1020−1022	−2.14	-	-
1030−1032	−2.09	-	-
1040−1042	−2.12	0.480	0.331
1050−1052	−1.97	-	-
1060−1062	−2.18	-	-
1070−1072	−2.03	-	-
1080−1082	−2.08	-	-
1090−1092	−2.07	0.470	0.305
1100−1102	−2.07	-	-
1110−1112	−2.13	-	-
1120−1122	−2.08	-	-
1130−1132	−2.06	1.050	0.267
MV-06			
0−2	−2.64	0.340	0.019
10−12	−2.58	0.260	0.017
20−22	−2.41	0.250	0.019
30−32	−2.53	0.230	0.017
40−42	−2.53	0.190	0.014
50−52	−2.40	0.380	0.027
60−62	−2.26	0.500	0.033
70−72	−2.21	0.620	0.044
80−82	−2.25	0.620	0.043
90−92	−1.80	0.370	0.026
100−102	−1.78	0.300	0.011

Table 1. (continued)

Sample Depth, cm	δ^{18}O, ‰	TOC, weight%	TOC MAR, g/cm²ka
	MV-07		
10−102	−1.71	-	-
20−22	−1.10	0.240	0.007
30−32	−0.87	0.290	0.021
40−42	−1.26	0.210	0.017
50−52	−1.33	0.260	0.007
60−62	−1.26	0.320	0.009
70−72	−1.55	0.340	0.009
80−82	−1.44	0.390	0.011
90−92	−1.59	0.370	0.008
100−102	−1.57	0.390	0.009
110−112	−1.65	0.440	0.010
120−122	−1.51	0.390	0.007
130−132	−1.61	0.350	0.007
140−142	−1.63	0.330	0.007
150−152	−1.79	-	-
160−162	−1.63		
170−172	−1.75		-
180−182	−1.71		-
190-192	−1.63	-	-
200−202	−1.42	0.390	0.030
210−212	−1.33	-	-
220−222	−1.26	0.340	0.021
230−232	−1.30	-	-
240−242	−1.37	0.380	0.024
250−252	−1.34	-	-
260−262	−1.44	0.400	0.024
270−272	−1.53	-	-
280−282	−1.87	0.370	0.023
290−292	−1.29	0.530	0.123
300−302	−1.65	-	-
310−312	−1.82	-	-
320−322	−2.00	-	-
330−332	−1.90	0.530	0.116
340−342	−2.05	-	-
350−352	−1.95	-	-
360−362	−2.27	-	-
370−372	−1.95	-	-
380−382	−2.15	-	-
390−392	−1.88	0.450	0.096
400−402	−1.99	-	-
410−412	−1.84	-	-
420−422	−1.58	-	-
430−432	−1.81	-	-
440−442	−1.90	0.450	0.114
450−452	−1.82	-	-
460−462	−1.80	-	-
470−472	−1.86	-	-
480−482	−1.68	-	-
490−492	−1.82	0.320	0.082
500−502	−1.96	-	-
510−512	−1.95	-	-
520−522	−1.93	-	-
530−532	−1.90	-	-
540−542	−2.07	0.340	0.070
550−552	−2.04	-	-
560−562	−1.91	-	-
570−572	−1.84	-	-
580−582	−1.74	-	-
590−592	−1.86	0.260	0.071
600−602	−2.16	-	-
610−612	−2.18	-	-
620−622	−1.96	-	-
630−632	−1.94	-	-
640−642	−2.05	0.430	0.190
650−652	−2.08	-	-
660−662	−1.89	-	-
670−672	−2.06	-	-
680−682	−2.23	-	-
690−692	−1.99	0.360	0.131
700−702	−2.16	-	-
710−712	−1.94	-	-
720−722	−2.14	-	-

Table 1. (continued)

Sample Depth, cm	δ^{18}O, ‰	TOC, weight%	TOC MAR, g/cm²ka
730−732	−1.82	-	-
740−742	−2.03	0.410	0.176
750−752	−1.89	-	-
760−762	−1.86	-	-
770−772	−1.95	-	-
780−782	−2.04	-	-
790−792	−2.30	0.440	0.190
800−802	−2.20	-	-
810−812	−2.10	-	-
820−822	−1.92	-	-
830−832	−1.89	-	-
840−842	−1.65	0.360	0.135
850−852	−2.06	-	-
860−862	−1.85	-	-
870−872	−2.01	-	-
880−882	−2.09	-	-
890−892	−1.90	0.370	0.171
900−902	−1.88	-	-
910−912	−1.96	-	-
920−922	−2.11	-	-
930−932	−2.00	-	-
940−942	−2.01	0.400	0.181
950−952	−2.21	-	-
960−962	−1.91	-	-
970−972	−2.17	-	-
980−982	−1.92	-	-
990−992	−2.22	0.430	0.163
1000−1002	−2.11	-	-
1010−1012	−2.06	-	-
1020−1022	−1.88	-	-
1030−1032	−1.97	-	-
1040−1042	−1.89	0.370	0.164
1050−1052	−2.17	-	-
1060−1062	−1.92	-	-
1070−1072	−1.92	-	-
1080−1082	−2.22	-	-
1090−1092	−1.76	0.330	0.148
1100−1102	−1.50	-	-
1110−1112	−1.88	-	-
1120−1122	−1.85	-	-
1126−1128	−1.80	0.290	0.039

[a]Isotope values are reported in delta notation relative to V-PDB.

75 m below modern sea level. The LGM is followed by a relatively rapid, though punctuated, sea level transgression, which culminates in the present sea level highstand by ∼6 ka.

3. Samples and Methods

3.1. Sediment Cores

[10] Two piston cores, MV24-0403-74JPC (MV-74) and MV26-0403-07JPC (MV-07), and one trigger gravity core, MV24-0403-06GC (MV-06), from southern Ashmore Trough were examined in this study (Figure 1). All three cores were taken during the PANASH cruise of RV *Melville* in March and April, 2004. MV-74 was retrieved in 684 m water depth from the steep upper slope (10.73°S, 144.08°E) 8 km east of the Great Barrier Reef. MV-07 and MV-06 were retrieved in 773 m water depth at the same location (10.44°S, 144.31°E), about 35 km to the northeast of MV-74 and at about mid distance (30 km) between the GBR and the southern tip of Ashmore Reef. Both piston cores are 11.3 m long, while the gravity core is 2.6 m long. The cores consist of varying amounts of siliciclastic

Table 2. Conventional and Corrected [14]C Years Before Present[a]

Sample Depth, cm	[14]C Ag, BP	Corrected [14]C Age, Cal years BP
MV-06		
10−12	1680 ± 25	1278 ± 20
80−82	9265 ± 20	10080 ± 89
MV-07		
10−12	11295 ± 25	12865 ± 78
50−52	26710 ± 140	21412 ± 32
120−122	39300 ± 360	43291 ± 445
MV-74		
10−12	2215 ± 20	1819 ± 31
100−102	8095 ± 25	8534 ± 33
150−152	9825 ± 25	10719 ± 36
165−167	11005 ± 25	12632 ± 35
235−237	37420 ± 270	42001 ± 175

[a]Corrected ages account for marine reservoir effects using CALIB 5.0.2 [*Stuiver and Reimer*, 1993], and secular variations in ^{14}C using an online calibration program [*Fairbanks et al.*, 2005].

material and pelagic and neritic carbonate [*Francis et al.*, 2006].

3.2. Sampling and Processing

[11] All whole cores were run through a GeoTek Sensor Core Logger at Louisiana State University to obtain physical properties data (e.g., fractional porosity, impedance, magnetic susceptibility, density P wave velocity, P wave amplitude). They were then split and sampled at 10-cm intervals. Bulk samples were freeze dried to remove pore water. Small portions of dried bulk samples were crushed with mortar and pestle, and reserved for certain analyses (e.g., organic carbon content). The remaining dried samples were weighed, placed in a solution of buffered hydrogen peroxide to remove organic matter, and sonicated to disaggregate grains (especially small calcite or calcareous ooze particles adhering to foraminiferal tests). All samples were then wet sieved over a 63-μm mesh sieve to separate coarse (>63 μm) and fine (<63 μm) components, and dried overnight in an oven at approximately 60°C. The coarse component was weighed and its mass was subtracted from the mass of the bulk sample to determine the percentage of coarse and fine components. Subsamples of the coarse component, obtained by dry sieving the sediment over various sieve sizes (e.g., 150 μm, 250 μm, and 300 μm), were examined using a Leica MZ6 stereomicroscope and used to extract foraminifera.

3.3. Oxygen Isotope and Radiocarbon Analyses

[12] Between four and eight specimens of the planktic foraminifer *Globigerinoides ruber* (white) were picked from the 250- to 300-μm-size fraction of every sample for isotopic analyses. Specimens with obvious indications of dissolution (e.g., partial tests and/or holes in tests) and secondary calcification were rejected. Stable oxygen and carbon isotope analyses were performed at the University of California, Davis using a GV Instruments Optima mass spectrometer. Isotope values are reported in delta notation relative to V-PDB (Table 1), and have an analytical precision of ±0.05‰ for $\delta^{18}O$ and ±0.0‰ for $\delta^{13}C$ (D. Winter, personal communication, 2006).

[13] Accelerator mass spectrometry (AMS) radiocarbon analysis was performed on five sediment samples from each of the MV-74 and MV-07/06 cores. Approximately 8 to 12 mg of mixed planktic foraminifers (*Globigerinoides ruber* and *Globigerinoides sacculifer*, representing ~500 to 600 tests) were picked from the >150-μm fraction using a binocular microscope. The foraminifer batches were sonicated in deionized water, and excess water and suspended particles were removed by pipette. Specimens with obvious dissolution features and secondary calcite were rejected. Analyses were performed at the University of California, Irvine AMS facility. Ages are reported as conventional ^{14}C years before present and as corrected calendar years (Table 2). Corrected ages account for marine reservoir effects using CALIB 5.0.2 [*Stuiver and Reimer*, 1993], and secular variations in ^{14}C using an online calibration program [*Fairbanks et al.*, 2005].

3.4. Total Organic Carbon Analyses

[14] Total organic carbon (TOC) contents (wt%) were determined on ~0.8-g samples of crushed bulk sediment taken every 10 to 50 cm down all three cores (Table 1). The sampling interval was varied because the stratigraphy indicates major changes in sedimentation rate, and we wanted to obtain a sufficient number of representative samples across variations in time and lithologies. Analyses were performed using a LECO C230 TOC Analyzer at Baseline Resolution Analytical Laboratories, Houston, Texas, with analytical precision of 0.01 wt%.

### 3.5. Foraminiferal Assemblages

[15] A microsplitter was used to obtain subsamples from the >150-μm-size fraction of selected samples. These subsamples were distributed across a gridded tray from which approximately 300 benthic tests were picked from random squares and identified under a binocular microscope. Key benthic taxa were identified to species level, while remaining taxa were divided into genera or distinct groups (Appendix A). The abundance (percent of population) of various species and groups were determined relative to the benthic population. Additionally, the abundance of benthic and planktic tests was determined relative to the total foraminiferal populations. Samples used for foraminiferal population analyses were chosen to represent the full ranges of eustatic sea level, siliciclastic and carbonate fluxes, and organic carbon contents. Although at fairly low sample resolution, foraminiferal population analyses presented here clearly change in concert with variations in these parameters.

3.6. Statistical Analysis

[16] The relative abundance data of benthic foraminifera were analyzed by R-mode (species versus species) principal component analysis (PCA) and Q-mode (sample versus sample) cluster analysis. Only key species, those that accounted for >2% of the population in at least one sample, were used (Appendix A). Multivariate analyses were performed using SAS 9.1 procedures (SAS Institute Inc., SAS OnlineDoc 9.1, 2003, available at http://support.sas.com/91doc/docMainpage.jsp) (hereinafter referred to as SAS Institute online documentation).

[17] The goals of the two statistical methods differ. PCA determines correlated variables (components) that account for as much data variance as possible [*Harman*, 1976] and is
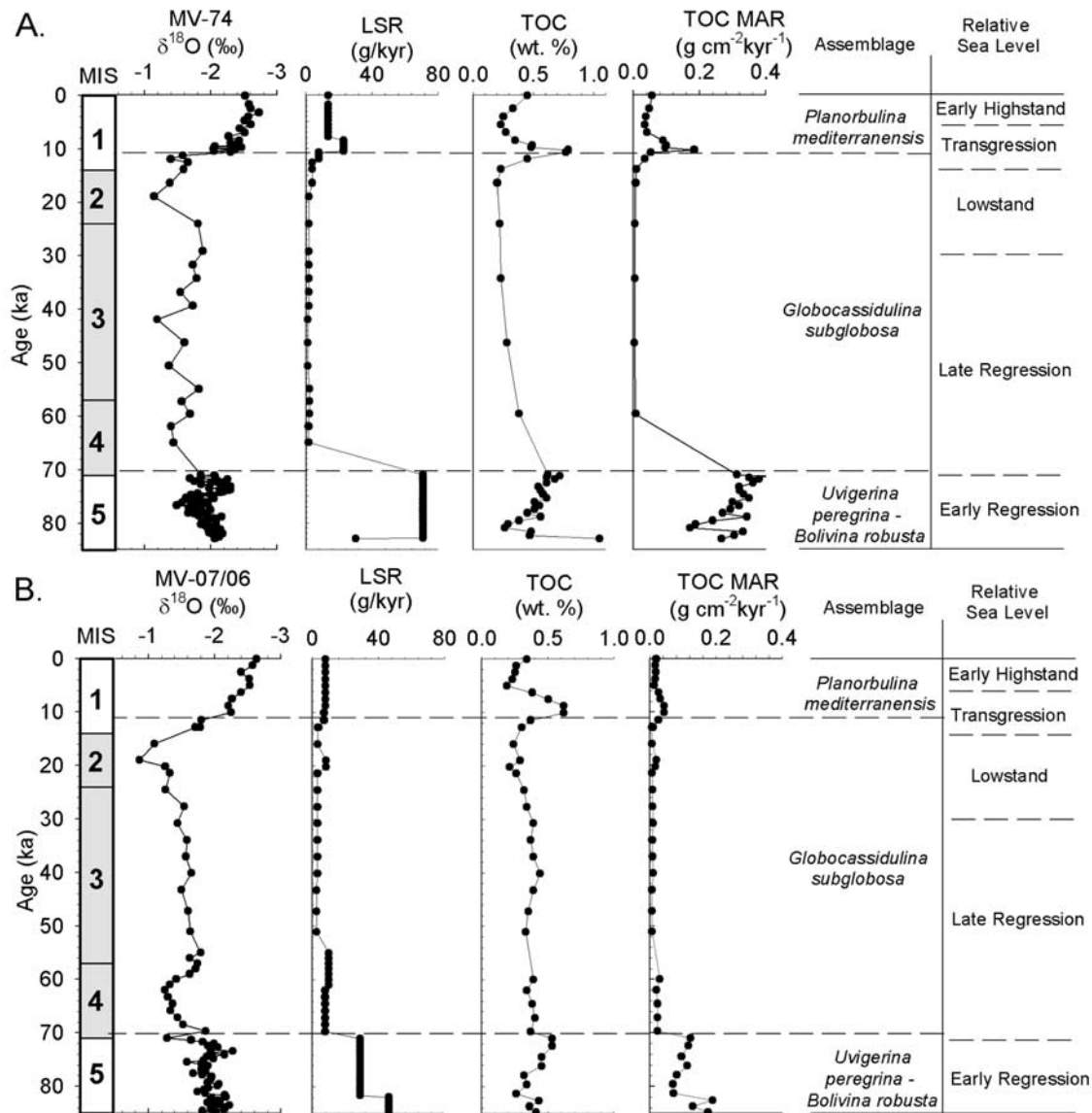
Figure 4. Linear sedimentation rates (LSRs), total organic carbon (TOC) content, and TOC Mass accumulation rates (MARs) shown with oxygen isotope records and MIS boundaries for (a) MV-74 and (b) MV-07/06.

particularly well suited for R-mode analyses [*Parker and Arnold*, 1999]. Significant components were identified by evaluation of the eigenvalue scores for each component [*Parker and Arnold*, 1999]. By contrast, cluster analysis separates data into groups that are relatively homogenous and distinct from other groups [*Davis*, 1986]. Several cluster procedures were employed, including Ward's minimum variance method, unweighted paired group method with arithmetic averaging (UPGMA or average linkage), and weighted paired group method (WPGMA or centroid). For each set of analyses, very similar results were obtained using the three clustering methods. It is assumed, therefore, that clusters are true representations of the data rather than artifacts of clustering procedures. Significant clusters were identified on the basis of cluster

dendrograms and pseudo-t^2 statistics (SAS Institute online documentation).

4. Results

4.1. Sediment Composition

[18] Cores used in this study (MV-74 and MV-07/06) consist of hemipelagic ooze and mud comprising siliciclastic material and pelagic and neritic carbonate. The coarse fraction (>63 μm) varies between 1 and 44% of the total sediment, and is dominated by pelagic carbonate (primarily planktic foraminifers and pteropods) with various amounts of benthic microfossils (benthic foraminifers, ostracods), echinoderm fragments, and sponge spicules. Siliciclastic material is minimal in the coarse fraction but abundant in the fine fraction (<63 μm), especially in samples from lower

depth intervals of the cores. Carbonate content in the fine fraction can be as high as 90% and as low as 5% [*Francis et al.*, 2006]. Carbonate material in the fine fraction includes aragonite, high magnesium calcite, and low magnesium calcite. In general, the abundance of aragonite and high magnesium calcite is greatest in the upper 0.5 to 1.5 m [*Francis et al.*, 2006].

4.2. Chronostratigraphy

[19] Chronologies for the two piston cores were established using the planktic foraminiferal oxygen isotope values (Table 1) and the corrected radiocarbon ages (Table 2). Prominent down core excursions in $\delta^{18}O$ from MV-74 and MV-07/06 were correlated to those of a well-dated stacked benthic oxygen isotope curve [*Lisiecki and Raymo*, 2005], as well as the planktic oxygen isotope record of a 36.5-m core that represents a full glacial cycle (or the last ~140 ka) taken in Ashmore Trough, MD05-2949 [*Jorry et al.*, 2008]. The oxygen isotope record for MV-07 demonstrates that sediment deposited between ~12.9 ka and the present is missing. Therefore a more complete oxygen isotope record for this location was obtained using samples from MV-06 (trigger core for the coring operation of piston core MV-07) and splicing the component records together. Sediment recovered at MV-74 and at MV-07/06 represents the last 83 ka and 93 ka, respectively (Figure 3).

4.3. Sediment and Organic Carbon Accumulation

[20] The TOC content varies between 0.2 and 1.1% in MV-74, and between 0.2 and 0.6% in MV-07/06 (Figure 4). For both cores, the highest TOC values are found in sediment deposited between ~75 and 70 ka, and between ~10.5 and 8.5 ka.

[21] The accumulation rate of sediment components, including organic carbon, can be calculated by

$$MAR_{TOC} = X(wt\%)*LSR*\rho_{db},$$

where X is the component of interest (e.g., TOC), LSR is the linear sedimentation rate, and ρ_{db} is the dry bulk density. LSRs can be determined over discrete intervals down cores by dividing thicknesses of sediment by the time they represent. LSRs varied between 1.7 and 80 cm/ka in MV-74, and between 2.6 and 47 cm/ka in MV-07/06 (Figure 4). In both cores, the highest LSRs occurred between ~83 and 70 ka (end of MIS 5, or MIS 5.1), while low to moderate LSRs characterize the remaining records. The ρ_{db} can be determined by

$$\rho_{db} = \rho_{bulk} - (FP*\rho_{water}),$$

where bulk density (ρ_{bulk}) and fractional porosity (FP) are measured on the GeoTek Core Logger, and 1.025 g/cm³ is the average density of seawater (ρ_{water}).

[22] MARs of TOC also changed significantly over the last ~83 ka, varying between 0.003 to 0.4 g cm⁻² ka⁻¹ in MV-74 and 0.007 to 0.2 g cm⁻²ka⁻¹ in MV-07/06 (Figure 4). The highest TOC accumulations occur between ~83 and 70 ka (MIS 5), while much lower accumulations characterize the remaining records. A prominent increase in TOC accumulations is observed at ~10.5 and 8.5 ka in both cores. Organic carbon MARs generally fluctuate in parallel
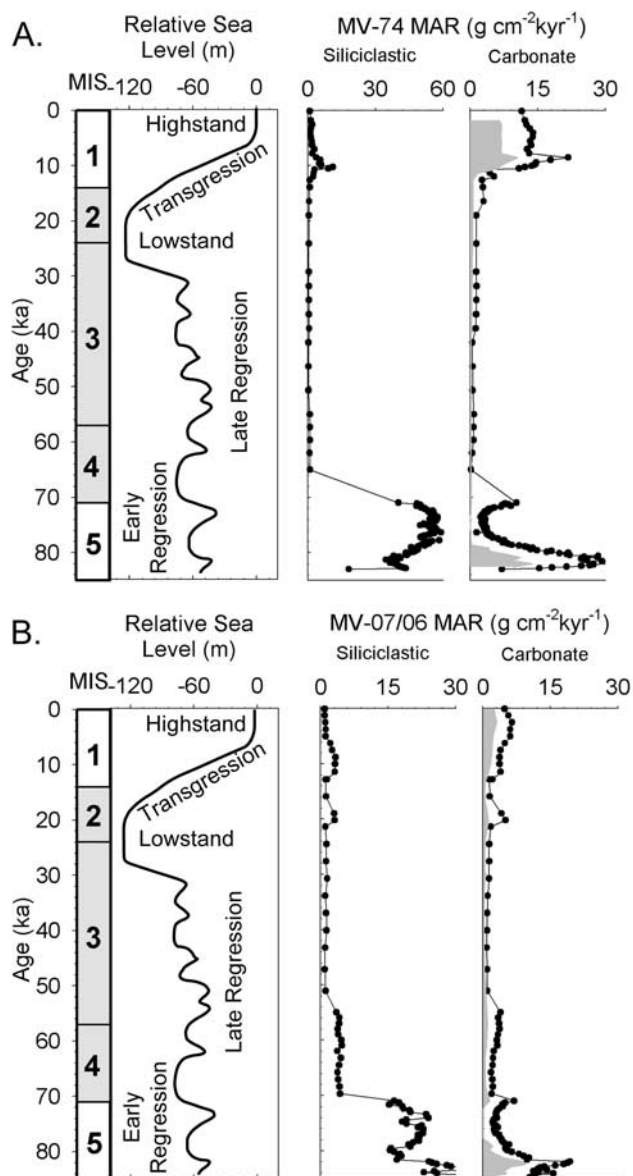

Figure 5. Mass accumulation rates (MARs) of bulk siliciclastic sediment and bulk carbonate sediment for (a) MV-74 and (b) MV-07/06 [from *Francis et al.*, 2006]. The shaded gray region of the bulk carbonate accumulation represents the accumulation of fine aragonite (<63 μm) sediment. Sediment accumulations are shown with a relative sea level curve for the last glacial cycle [from *Lambeck et al.*, 2002], as well as oxygen isotope records and MIS boundaries.

with siliciclastic MARs (Figure 5), which were calculated using data presented elsewhere [*Francis et al.*, 2006].

4.4. Foraminiferal Assemblages

4.4.1. General Overview

[23] Throughout the study interval, planktic taxa are more abundant than benthic taxa, accounting for between 55 and 95% of the total foraminiferal assemblages in MV-74, and between 83 and 97% of the total foraminiferal assemblages in MV-07/06 (Figure 6). The highest planktic (and lowest benthic) abundances occur in sediment deposited between
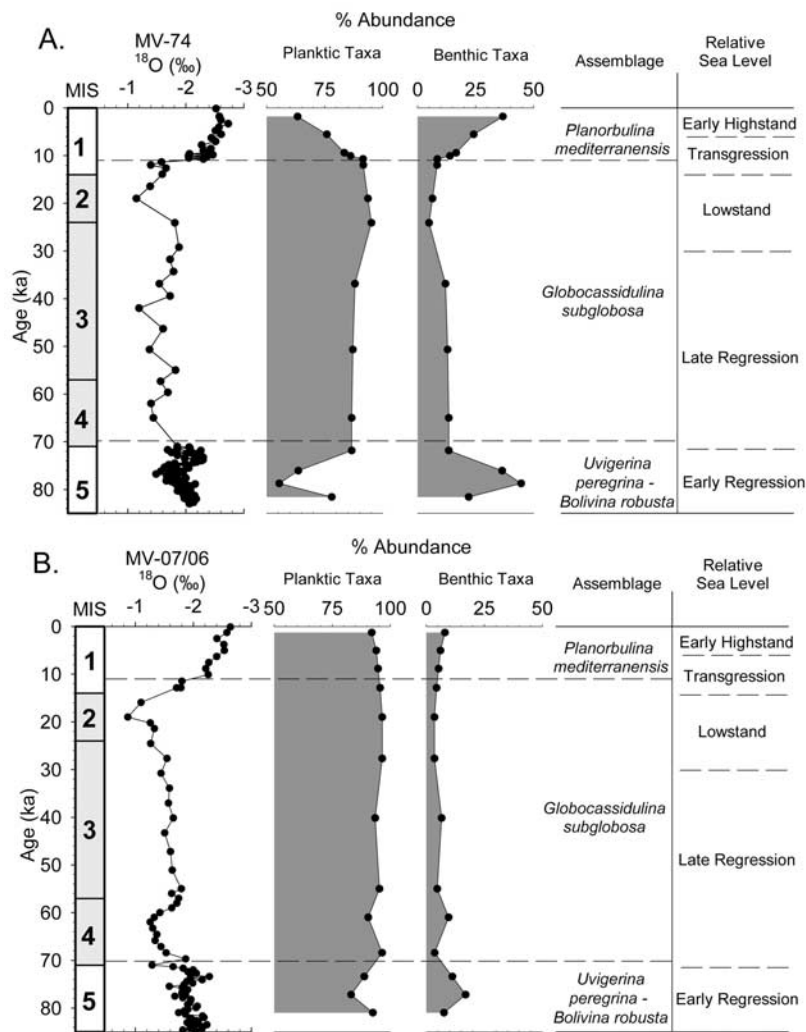
Figure 6. Planktic taxa abundances relative to the entire foraminiferal populations (planktic + benthic taxa) and the abundances of calcareous benthic taxa relative to the entire benthic populations shown with oxygen isotope records and MIS boundaries for (a) MV-74 and (b) MV-07/06. Also indicated are the benthic foraminiferal assemblages determined by this study, as well as generalized relative sea level.

~70 and 11 ka (i.e., late regression through lowstand and early transgression).

[24] Benthic assemblages contain diverse mixtures of taxa that inhabit shelf to lower slope settings, and epifaunal to deep infaunal microhabitats. Calcareous forms (as opposed to agglutinated forms) dominate benthic assemblages, accounting for 88% or greater of the benthic populations in both cores (Figure 6).

[25] Benthic taxa of key importance were determined by evaluation of down core relative abundances and PCA (Appendix A) and include *Uvigerina peregrina*, *Bolivina robusta*, *Sphaeroidina bulloides*, *Bulimina marginata*, *Globocassidulina subglobosa*, *Globocassidulina* cf. *G. subglobosa*, *Siphouvigerina porrecta*, *Planorbulina mediterranensis*, *Rosalina* spp. + *Discorbis* spp., *Reussella hayasakai*, and species of the family Miliolidae. Benthic relative abundances and multivariate techniques indicate three well-defined benthic foraminiferal assemblages. These assemblages are named for their most diagnostic taxa: *Uvigerina peregrina-Bolivina robusta*, *Globocassidulina subglobosa*, and *Planorbulina mediterranensis*.

4.4.2. Down-Core Benthic Relative Abundances

[26] The relative abundances of key benthic taxa change significantly over the time represented by MV-74 (Figure 7) and MV-07/06 (Figure 8). *Uvigerina peregrina* and *Bolivina robusta* occur in low abundances, except in sediment deposited between 83 and 70 ka (early regression), where they are as high as 37% and 19% of the benthic populations, respectively. *Sphaeroidina bulloides* and *Bulimina marginata* also have increased abundances in this interval. *Globocassidulina subglobosa*, which represents 0–14% of the benthic assemblages down the cores, has its highest abundances between 70 and 11 ka (late regression through lowstand and early transgression). *Globocassidulina* cf. *G. subglobosa* is most abundant in MV-07/06, and its relative abundance generally tracks that of *Globocassidulina subglobosa*. In MV-74, *Planorbulina mediterranensis* has a low abundance in most sediment (<3%), with the exception of that deposited from 11 ka to the present (late transgression through early highstand), where it reaches 20%. A similar, though less pronounced increase is observed in MV-07/06. In all three cores, peak abundances of the *Rosalina*
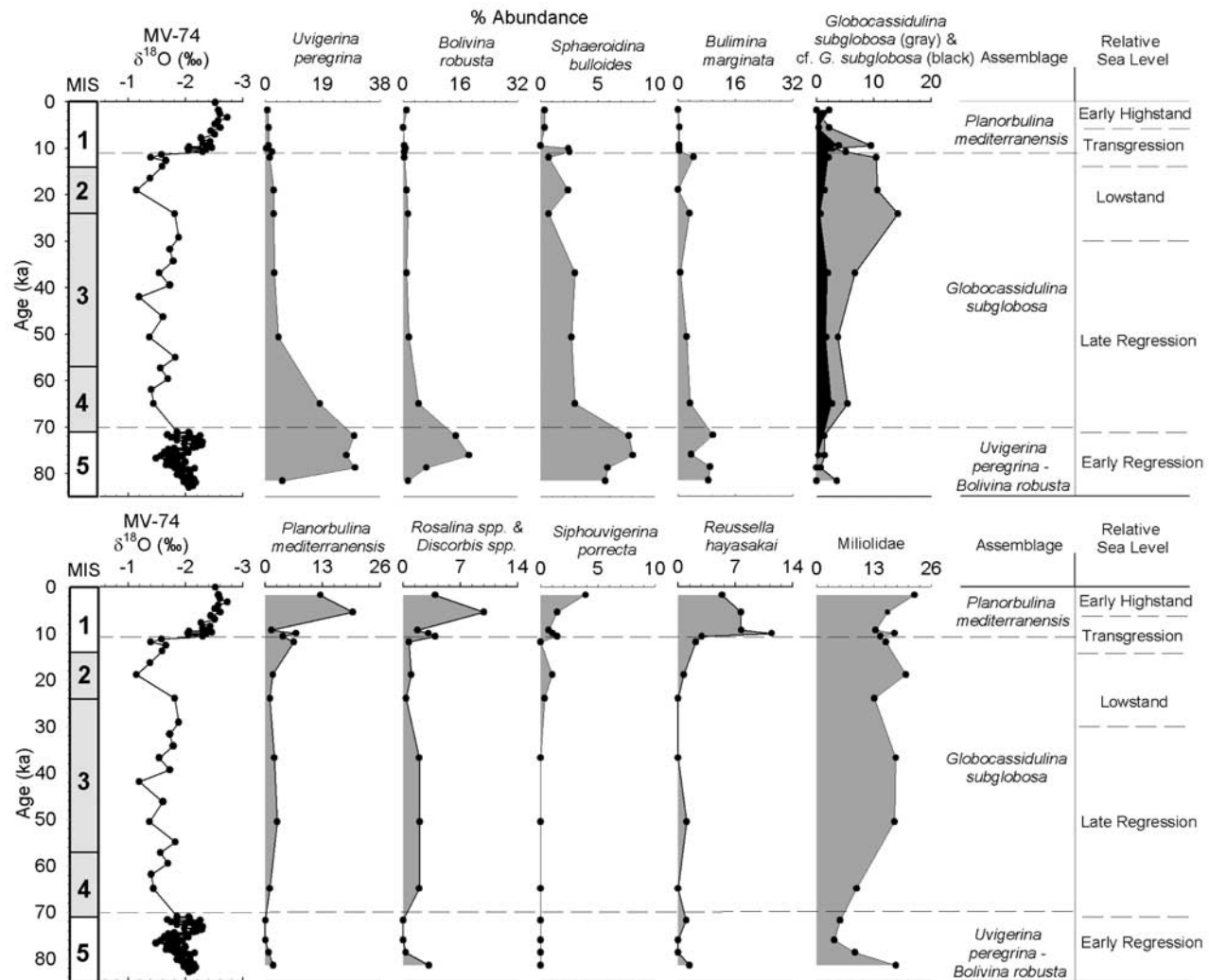
Figure 7. MV-74 key benthic taxa abundances relative to the entire benthic population shown with the oxygen isotope record and MIS boundaries. Also indicated are the benthic foraminiferal assemblages determined by this study, as well as generalized relative sea level.

spp. + *Discorbis* spp. group and *Reussella hayasakai* coincide with peak abundances of *Planorbulina mediterranensis* during late transgression and early highstand. *Siphouvigerina porrecta* accounts for 1% or less of the benthic populations in sediment deposited before ~9 ka, but upward of 6% in uppermost sediment. Miliolidae abundances range between ~11 and 22% of the benthic populations in all cores, with the exception of very low abundances (4–9%) in sediment deposited between ~83 and 70 ka.

4.4.3. Benthic Multivariate Analyses

[27] Statistical analyses illuminate these down core changes in benthic foraminiferal assemblages. R-mode PCA reveals two significant components, while Q-mode cluster analysis reveals three significant clusters. This is true for both MV-74 (Table 3 and Figure 9) and MV-07/06 (Table 4 and Figure 10).

[28] At both locations, R-mode "component 1" explains most (~65–72%) of the variance. It is dominated by strong positive loadings of *Uvigerina peregrina* and *Bolivina robusta*. In MV-74, *Sphaeroidina bulloides*, *Bulimina marginata*, and *Cassidulina teretis* are also common to this

component, while *Planorbulina mediterranensis*, *Globocassidulina subglobosa*, and *Reussella hayasakai* have negative loadings. Samples defined by R-mode "component 1" are typically associated with samples that fall into Q-mode "cluster A". We refer to this as the *Uvigerina peregrina-Bolivina robusta* assemblage owing to the dominance of these two species, and it characterized by samples dated between ~80 and 70 ka (early regression).

[29] R-mode "component 2" explains ~13% of the variance in MV-74. It is characterized by high positive loadings of *Planorbulina mediterranensis* and to a lesser extent *Reussella hayasakai*, and strong negative loadings of *Globocassidulina subglobosa*. Samples defined by this component are associated with those defined by Q-mode "cluster C". We refer to this as the *Planorbulina mediterranensis* assemblage. Although this assemblage was not distinguished by R-mode PCA in MV-07/06, Q-mode cluster analysis identified "cluster C" in this core, which also principally occurs in samples dated from ~11 ka to the present (late transgression through early highstand).
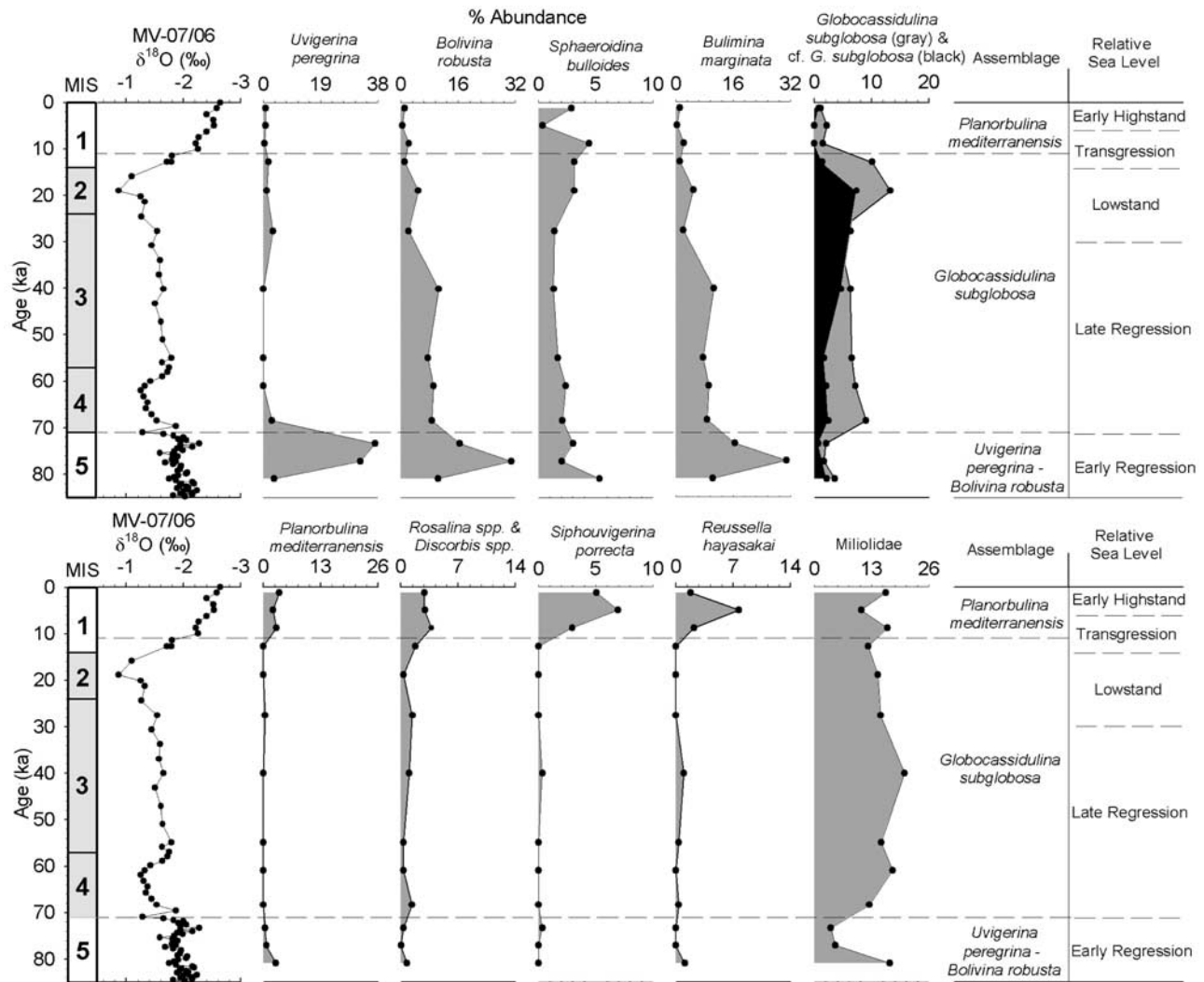
Figure 8. MV-07/06 key benthic taxa abundances relative to the entire benthic population shown with the oxygen isotope record and MIS boundaries. Also indicated are the benthic foraminiferal assemblages determined by this study, as well as generalized relative sea level.

Table 3. Benthic MV-74 R-Mode PCA Significant Component Loadings

Benthic Species	Component 1	Component 2
Amphistegina lessonii	−0.022625	0.055093
Aphelophragmina semilineata	0.002444	−0.029627
Bolivina compacta	−0.032077	0.147248
Bolivina robusta	0.361842	0.088798
Bolivinitia quadrilatera	0.03542	−0.013055
Bulimina aculeata	0.010368	−0.036489
Bulimina marginata	0.182029	−0.044191
Bulimina striata	−0.001474	−0.065741
Cassidulina teretis	0.204252	−0.013288
Ehrenbergina pacifica	−0.043276	−0.042675
Eggerella bradyi	−0.011137	−0.013067
Globocassidulina crassa	−0.042077	−0.055179
Globocassidulina subglobosa	−0.155347	−0.521215
Globocassidulina c.f. *subglobosa*	−0.029293	−0.038791
Globocassidulina c.f. *elegans*	−0.015962	−0.099132
Gyroidina altiformis	−0.024265	−0.000916
Gyroidina obicularis	−0.019195	−0.009459
Gyroidina sp.	0.015807	−0.016297
Hoeglundina elegans	−0.017461	−0.023303
Hyalinea baltica	−0.017957	−0.036043
Melonis barleeanus	−0.009992	−0.048459
Melonis pompilioides	−0.011312	−0.014189
Neouvigerina ampullacea	0.056094	−0.051599
Oridorsalis tener	0.00434	−0.019083
Planorbulina mediterranensis	−0.211476	0.74463
Pullenia bulloides	0.010674	−0.065032
Pullenia subcarinata	−0.004056	−0.013203
Rectobolivina bifrons	0.044887	0.0002
Reussella hayasakai	−0.109997	0.266749
Sigmavirgulina turtosa	−0.05902	0.059443
Sigmoilina schlumbergeri	0.087092	−0.009172
Siphogenerina pacifica	0.007422	−0.047729
Siphonina bradyana	−0.040236	0.021277
Siphouvigerina porrecta	−0.037279	0.10464
Sphaeroidina bulloides	0.173834	−0.020119
Uvigerina peregrina	0.808547	0.122571

[30] MV-07/06 R-mode "component 2" explains ∼10% of the variance and expresses positive loadings of *Globocassidulina subglobosa*, *Globocassidulina* cf. *G. subglobosa*, and *Bolivina robusta*. Negative loadings are shown by *Siphouvigerina porrecta*, *Uvigerina peregrina*, *Reussella hayasakai*, and *Planorbulina mediterranensis*. These samples typically fall into "cluster B". We refer to this assemblage as the *Globocassidulina subglobosa* assemblage, and it is characterized by samples dated from ∼71 to 11 ka, as well as a sample from ∼81 ka (late regression through early transgression).

## 5. Discussion

5.1. Organic Carbon

[31] Accumulation of organic carbon (Figure 4) and siliciclastic material (Figure 5) have fluctuated in parallel on the slopes of Ashmore Trough. The greatest organic carbon and siliciclastic fluxes occurred between ∼83 and 70 ka (early regression), and between ∼10.5 and 8.5 ka (transgression). These intervals of high siliciclastic delivery likely reflect remobilization and redeposition of sediments previously deposited on the shelf, direct input of fluvial material to the outer shelf and upper slope, or both [*Jorry et al.*, 2008; *Francis et al.*, 2006]. In either case, terrestrial organic carbon delivery to slopes of Ashmore Trough would have also increased. Additionally, riverine delivery of

nutrients during intervals of increased fluvial discharge potentially heightened surface water productivity, elevating marine organic carbon flux to the seafloor. Generally low organic carbon accumulations occur between ∼70 and 11 ka. This is when siliciclastic delivery to slopes of Ashmore Trough was at a minimum, perhaps because fluvially derived material bypassed slopes to deeper parts of the GoP [*Francis et al.*, 2006]. Most of the Holocene record (∼8.5 to 0 ka) is characterized by low to moderate organic carbon accumulation, corresponding to an interval of low to moderate siliciclastic accumulation. During this interval of sea level highstand, most fluvially derived sediment has remained on the shelf [*Walsh and Nittrouer*, 2003], although a small portion has leaked to the slopes of Ashmore Trough [*Francis et al.*, 2006].

[32] The flux of organic carbon to the seafloor and the dissolved oxygen concentrations in bottom water and shallow sediments are limiting resources for benthic foraminiferal communities [e.g., *Gooday*, 1988; *Jorissen et al.*, 1995; *Thomas and Gooday*, 1996; *Schmiedl et al.*, 1997; *Jorissen*, 1999; *Loubere and Fariduddin*, 1999]. These factors are also related, as high organic carbon inputs to the seafloor lead to microbial consumption of dissolved oxygen at or immediately below the sediment-water interface [e.g., *Jorissen et al.*, 1995; *Bernhard and Sen Gupta*, 1999; *Loubere and Fariduddin*, 1999]. Consequently, it is hard to distinguish the relative influence of these parameters on infaunal community structure [e.g., *Jorissen et al.*, 1992; *Jorissen*, 1999; *Loubere and Fariduddin*, 1999]. Nonetheless, some combination of organic carbon flux and dissolved oxygen concentrations appears to strongly influence benthic foraminiferal populations in sediment on slopes of Ashmore Trough.

5.2. *Uvigerina peregrina-Bolivina robusta* Assemblage (Early Regression)

[33] The *Uvigerina peregrina-Bolivina robusta* benthic foraminiferal assemblage is the most distinct foraminiferal assemblage recognized in Ashmore Trough through the study interval. This assemblage is most prevalent between ∼83 and 70 ka (early regression), an interval when organic carbon accumulations were the highest on the slopes of Ashmore Trough (Figure 4). Taxa characterizing this group are typically shallow infaunal species with tests of high surface-to-volume ratio and ornamented walls (i.e., *Uvigerina peregrina*), or with tests of flattened elongated shapes containing abundant pores (i.e., *Bolivina robusta*). These elongate test morphologies are associated with infaunal lifestyles and environments characterized by high organic carbon flux [*Corliss and Chen*, 1988; *Corliss and Fois*, 1990; *Rosoff and Corliss*, 1992; *Jorissen et al.*, 1995; *Jorissen*, 1999; *Loubere and Fariduddin*, 1999], and/or dysoxic to anoxic conditions on the seafloor or within the seafloor sediments [e.g., *Kaiho*, 1994, 1999; *Bernhard and Sen Gupta*, 1999]. In particular, *Uvigerina peregrina* is a common and well documented bathyal species that is associated with heightened organic carbon content [e.g., *Miller and Lohmann*, 1982; *Rathburn and Corliss*, 1994], elevated productivity [e.g., *Loubere*, 1994, 1998; *Loubere and Fariduddin*, 1999], and depleted bottom water oxygen concentration [e.g., *Lohmann*, 1978; *Kaiho*, 1994]. Studies involving well constrained ecologic parameters suggest that
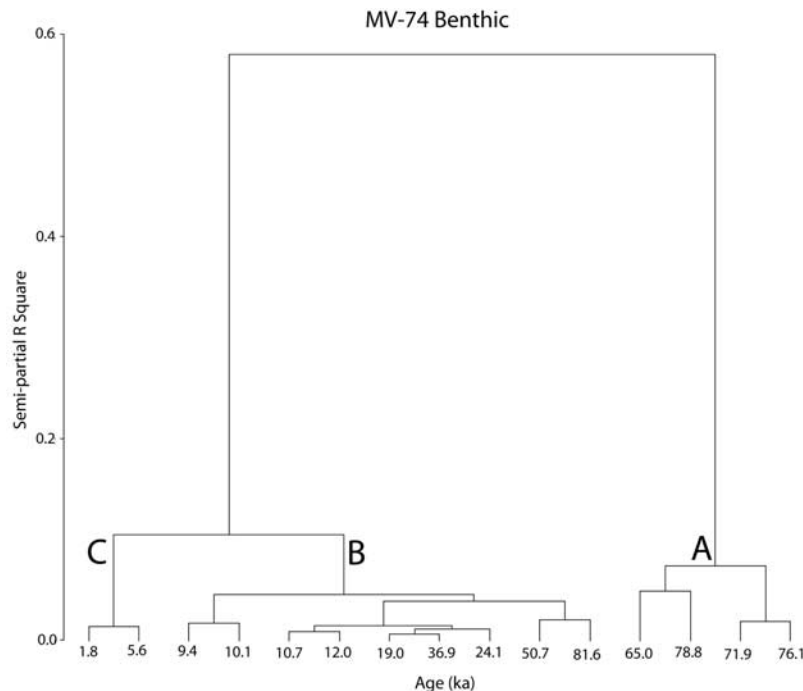
Figure 9. MV-74 benthic assemblage cluster diagram using Q-mode Ward's Minimum Variance method. The three significant benthic clusters determined by this study are indicated.

the distribution of *Uvigerina peregrina* is dominantly controlled by organic carbon supply and, secondarily, by oxygen levels [*Miller and Lohmann*, 1982; *Rathbun and Corliss*, 1994]. Studies have also associated *Bulimina marginata* and *Sphaeroidina bulloides*, common species of the *Uvigerina peregrina-Bolivina robusta* assemblage, with heightened productivity and/or low oxygen conditions [e.g., *Linke and Lutze*, 1993; *Mackensen et al.*, 1993; *Bernhard and Alve*, 1996; *Loubere*, 1996; *Jorissen et al.*, 1999]. In Ashmore Trough, the *Uvigerina peregrina-Bolivina robusta* assemblage appeared in response to heightened organic carbon flux to the seabed, associated with increased siliciclastic fluxes to the slopes (Figure 5), and perhaps with a concomitant decrease in oxygen concentrations in bottom water or shallow sediments.

5.3. *Globocassidulina subglobosa* Assemblage (Late Regression Through Lowstand and Early Transgression)

[34] The *Globocassidulina subglobosa* assemblage is most prevalent in Ashmore Trough between ∼70 and 11 ka (late regression through lowstand and early transgression), an interval when organic carbon fluxes were generally very low. *Globocassidulina subglobosa* is a broadly distributed species whose occurrence has been reported from the upper slope to abyssal plain [e.g., *Phleger and Parker*, 1951; *Poag*, 1981; *Murray*, 1991; *Loubere et al.*, 1988]. Its distribution has been associated with low organic carbon flux [e.g., *Loubere et al.*, 1998; *Gooday*, 1993; *Schmiedl et al.*, 1997], low productivity [e.g., *Loubere et al.*, 1988; *Loubere and Fariduddin*, 1999], or well-oxygenated bottom waters [e.g., *Murray*, 1991; *Schmiedl et al.*, 1997]. In Ashmore Trough, the *Globocassidulina subglobosa* assemblage appeared in response to the low organic carbon flux, associated with low siliciclastic input, to the seafloor or

well-oxygenated waters that developed at the sediment-water interface and/or within the sediments.

5.4. *Planorbulina mediterranensis* Assemblage (Late Transgression Through Early Highstand)

[35] The *Planorbulina mediterranensis* assemblage is characterized by an increase in genera typically associated with shallow (<200 m) shelf environments [e.g., *Phleger and Parker*, 1951; *Murray*, 1991; *Loeblich and Tappan*, 1994; *Leckie and Olson*, 2003]. The taxa exemplifying this assemblage are generally epifaunal, attached or temporally attached forms (e.g., *Planorbulina mediterranensis*, *Rosalina* spp. and *Discorbis* spp.) that prefer substrates found in nearshore waters such as seagrasses, corals, and shells [e.g., *Phleger and Parker*, 1951; *Phleger*, 1960; *Poag*, 1981; *Murray*, 1991; *Sen Gupta*, 1999b]. The *Planorbulina mediterranensis* assemblage prevails in Ashmore Trough sediment deposited from ∼11 ka to the present day (late transgression through early highstand). Significant off-shelf and off-bank transport of neritic carbonate during late transgression and highstand, often termed "highstand shedding", typifies tropical reef systems and carbonate platforms submerged within the photic zone [*Droxler and Schlager*, 1985; *Schlager et al.*, 1994], including the GBR [*Dunbar et al.*, 2000; *Page et al.*, 2003]. Indeed, this phenomenon appears to occur in Ashmore Trough, as indicated by large increases in the supply of fine-grained carbonate (Figure 5), primarily aragonite and high magnesium calcite, beginning ∼11 ka [*Francis et al.*, 2006] and corresponding to the initial reflooding of the shelf and bank tops; a calci-turbidite and onset of fine-grained aragonite also marks ∼11 ka in neighboring Pandora Trough [*Jorry et al.*, 2008]. Consequently, the *Planorbulina mediterranensis* assemblage likely indicates substantial displacement of benthic foraminifera produced on the GBR and offshore

Table 4. Benthic MV-07/06 R-Mode PCA Significant Component Loadings

Benthic Species	Component 1	Component 2
Amphistegina lessonii	−0.003234	−0.00739
Aphelophragmina semilineata	−0.000495	0.006704
Bolivina compacta	−0.000803	−0.016746
Bolivina robusta	0.502064	0.543894
Bolivinitia quadrilatera	0.032348	−0.035552
Bulimina aculeata	0.003472	0.003026
Bulimina marginata	0.070983	0.051883
Bulimina striata	−0.046883	−0.066219
Cassidulina teretis	0.013786	0.128336
Ehrenbergina pacifica	−0.088474	0.117865
Eggerella bradyi	−0.013437	0.088299
Globocassidulina crassa	−0.033275	−0.116491
Globocassidulina subglobosa	−0.096361	0.481112
Globocassidulina c.f. subglobosa	−0.032823	0.243017
Globocassidulina c.f. elegans	−0.001589	0.002693
Gyroidina altiformis	−0.022927	−0.054976
Gyroidina obicularis	−0.022975	−0.006014
Gyroidina sp.	−0.003695	0.038762
Hoeglundina elegans	0.007835	−0.009644
Hyalinea baltica	−0.022145	0.026986
Melonis barleeanus	−0.025164	0.145172
Melonis pompilioides	0	0
Neouvigerina ampullacea	−0.031213	0.118579
Oridorsalis tener	−0.004647	0.074115
Planorbulina mediterranensis	−0.016601	−0.168627
Pullenia bulloides	0.002159	0.073097
Pullenia subcarinata	−0.022748	0.008745
Rectobolivina bifrons	−0.006055	−0.004184
Reussella hayasakai	−0.042561	−0.248689
Sigmavirgulina turtosa	0	0
Sigmoilina schlumbergeri	0.028273	0.017641
Siphogenerina pacifica	−0.021352	−0.048015
Siphonina bradyana	−0.025287	−0.104693
Siphouvigerina porrecta	−0.045684	−0.337404
Sphaeroidina bulloides	0.002864	−0.002825
Uvigerina peregrina	0.842657	−0.28988

atolls in the GOP. Furthermore, the *Planorbulina mediterranensis* assemblage is more abundant at MV-74, located on the steep upper slope, proximal (8 km) to neritic carbonate sources (Figure 1) and where carbonate flux is greatest (Figure 5).

5.5. Benthic to Planktic Relative Abundances

[36] In sediment deposited in outer neritic to bathyal depths of the modern ocean, planktic taxa typically comprise >80% of the foraminiferal assemblage [e.g., *Gibson*, 1989; *Leckie and Olson*, 2003]. However, variations in organic carbon flux can alter the ratio of benthic to planktic foraminifera. Spurred by increased food supply, the relative abundance of benthic foraminifera increase with heightened organic carbon flux to the seafloor [e.g., *Diester-Haass*, 1978; *Berger and Diester-Haass*, 1988; *Herguera and Berger*, 1991]. This seems to be observed on slopes of Ashmore Trough. Relative abundances of benthic foraminifera were generally high between ∼83 and 70 ka, a time when the *Uvigerina peregrina-Bolivina robusta* assemblage dominates (Figures 7 and 8) and organic carbon fluxes to the slopes are greatest (Figure 4). By contrast, the lowest benthic relative abundances occurred between ∼70 and 11 ka, a time when the *Globocassidulina subglobosa* assemblage is most abundant (Figures 7 and 8) and organic carbon fluxes to the slopes are the lowest (Figure 4).

[37] The trend to higher relative abundances of benthic foraminifera from ∼11 ka to the present, particularly in MV-74, coincided with modest organic carbon flux and heightened carbonate flux. This observation can be explained by increased shedding of benthic foraminifera from the outer shelf and atolls, corresponding to reflooding of the shelf and bank tops and production of neritic sediments, typically containing higher relative abundances of benthic foraminifera [e.g., *Buzas and Gibson*, 1969; *Boltovskoy and Wright*, 1976; *Gibson*, 1989]. This is consistent with the dominance and composition of the *Planorbulina mediterranensis* assemblage in these sediments.

5.6. Summary

[38] Late Pleistocene to Holocene (∼83 ka to the present) benthic foraminiferal communities in Ashmore Trough are clearly influenced by changing organic carbon and sediment input along the margin. Previous studies have documented the influence of organic carbon flux to the seafloor on benthic foraminiferal communities, including the affinity of *Uvigerina peregrina* with high organic carbon flux [e.g., *Miller and Lohmann*, 1982; *Rathburn and Corliss*, 1994] and the association of *Globocassidulina subglobosa* with low organic carbon flux [e.g., *Loubere et al.*, 1988; *Gooday*, 1993; *Schmiedl et al.*, 1997]. Previous studies have also documented distinct differences in benthic foraminiferal species composition and abundance in purely siliciclastic and purely carbonate regions [e.g., *Poag*, 1981; *Murray*, 1991]. This study clearly documents the importance of both siliciclastic and carbonate components on the benthic foraminiferal populations adjacent the Ashmore Trough mixed siliciclastic-carbonate margin. The interplay of organic carbon flux, coupled with siliciclastic and carbonate sediment inputs along the margin significantly influences the benthic foraminiferal communities on the slope. Ashmore Trough provides an analogue for ancient mixed siliciclastic-carbon-
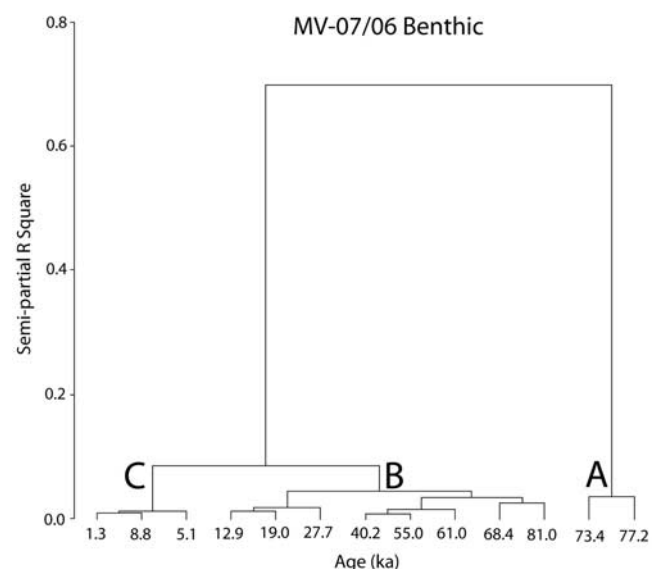
Figure 10. MV-07/06 benthic assemblage cluster diagrams using Q-mode Ward's Minimum Variance method. The three significant benthic clusters determined by this study are indicated.

Table A1. List of Key Benthic Taxa That Account for >2% of the Assemblages in at Least One Sample[a]

Taxa	Details	Description/Discussion
Agglutinated taxa	RA	species such as *Karreriella bradyi* Cushman, *Migros flintii* (Cushman), *Sahulia lutzei* Langer, *Siphotextularia mestayerae* Vella, *Siphotextularia foliosa* Zheng, and *Textularia conica* d'Orbigny are typical of this group
Amphistegina lessonii d'Orbigny	PCA, CA	
Aphelophragmina semilineata (Belford)	PCA, CA	test biserial, elongate, compressed, gradually tapered, perforate, longitudinal costae; differentiated from *Bolivina* by smoother surface and presence of costae
Bolivina compacta Sidebottom	PCA, CA	test biserial, elongate, compressed, gradually tapered, coarsely perforate; distinguished from *B. robusta* by more abundant pores and lack of terminal spine
Bolivina robusta Brady	RA, PCA, CA	test biserial, elongate, compressed, gradually tapered, coarsely perforate; well-developed terminal spine, variable in length
Bolivinita quadrilatera (Schwager)	PCA, CA	very distinct species; test biserial, elongate, broad chambers, box-like shape in peripheral view, well developed terminal spine
Bulimina aculeata d'Orbigny	PCA, CA	test triserial, inflated chambers, finely perforate, numerous spines covering early chambers and base of final chambers; shows significant variability in length and thickness of spines
Bulimina marginata d'Orbigny	RA, PCA, CA	test triserial, inflated chambers, finely perforate, distinct chamber margins rimmed with fairly uniform spines; distinguished from *B. aculeata* by distinct "ledge like" chamber margins containing shorter, more uniform spines
Bulimina striata d'Orbigny	PCA, CA	test triserial, inflated chambers, finely perforate, distinct longitudinal costae ending in tiny spines; distinguished from other species of *Bulimina* by costae
Cassidulina teretis Tappan	PCA, CA	
Cibicides spp.		species such as *Cibicides lobatulus* (Walker and Jacob) are typical of this group
Cibicidoides spp.		species such as *Cibicidoides bradi* (Trauth) and *Cibicidoides robertsoniansus* (Brady) are typical of this group
Eggerella bradyi (Cushman)	PCA, CA	
Ehrenbergina pacifica Cushman	PCA, CA	
Elphidium spp.		rare; however, typically occur with the *Planorbulina mediterranensis* assemblage
Globobulimina spp.		occurrence almost exclusively with the *Uvigerina peregrina-Bolivina robusta* assemblage
Globocassidulina crassa d'Orbigny	PCA, CA	test subspherical, flatted in periphery, perforate, with slit-like aperture; considerable range in size; distinguished from *G. subglobosa* by more flatted periphery and slit-like aperture
Globocassidulina subglobosa (Brady)	RA, PCA, CA	test subspherical, inflated chambers, perforate, with distinct loop-like aperture; considerable range in size
Globocassidulina cf. *G. subglobosa* (Brady)	RA, PCA, CA	this species very similar to *G. subglobosa*, but with a more slit-like aperture resembling that of *G. crassa* versus the typical loop-like aperture of *G. subglobosa*
Globocassidulina cf. *G. elegans* (Sidebottom)	PCA, CA	test subspherical, enrolled, inflated chambers, with distinct tiny thick spine-like ornamentation on sutures
Gyroidina altiformis Stewart & Stewart	PCA, CA	test biconvex, slightly convex dorsal side, and highly vaulted spiral side, finely perforate, numerous chambers
Gyroidina obicularis d'Orbigny	PCA, CA	test biconvex, slightly convex dorsal side, to moderately convex spiral side, finely perforate, numerous chambers; differentiated from *G. altiformis* by smoother test and less vaulted umbilical side
Gyroidina sp.	PCA, CA	similar to *Gyroidina altiformis*, but with fewer chambers (generally 5 to 6 chambers in final whorl)
Hoeglundina elegans (d'Orbigny)	PCA, CA	
Hyalinea baltica (Schrorter)	PCA, CA	
Melonis barleeanus (Williamson)	PCA, CA	
Melonis pompilioides (Fichtel and Moll)	PCA, CA	
Miliolidae	RA	this family includes a diverse array of species with porcellaneous tests
Nonionella spp.		
Nodosariidae		this family includes a diverse array of rare species
Neouvigerina ampullacea (Brady)	PCA, CA	test triserial, ovate, finely perforate, finely hispid, same as *Uvigerina ampullacea* Brady; distinguished from other uvigerinids by its finely hispid surface
Oridorsalis tener (Brady)	PCA, CA	
Planorbulina mediterranensis d'Orbigny	RA, PCA, CA	very distinct species; test discoidal, concavo-convex, coarsely perforate
Planulina spp.		species such as *Planulina bradyi* Tolmachoff and *Planulina wuellerstorfi* (Schwager) are typical of this group
Pullenia bulloides (d'Orbigny)	RA, PCA, CA	test planispiral, spherical, finely perforate, few chambers, narrow crescent-shaped aperture extending almost entirely from one side to the other
Pullenia subcarinata (d'Orbigny)	PCA, CA	test planispiral, compressed, finely perforate, few chambers. Similar to *P. bulloides*, but compressed
Rosalina spp. + *Discorbis* spp.	RA	includes a number of "attached" or "temporarily attached" species
Rectobolivina bifrons (Brady)	PCA, CA	
Reussella hayasakai Ôki	RA, PCA, CA	test triserial, triangular, gradually enlarging, coarsely perforate, raised sutures with fine spines extending from margins
Sigmavirgulina turtosa (Brady)	PCA, CA	test biserial, elongate, compressed, gradually twisting chambers, coarsely perforate with highest concentration of pores on latter chambers
Sigmoilina schlumbergeri (Silvestri)	PCA, CA	
Siphogenerina pacifica (Cushman)	PCA, CA	
Siphonina bradyana Cushman	PCA, CA	

Table A1. (continued)

Taxa	Details	Description/Discussion
Siphouvigerina porrecta (Brady)	RA, PCA, CA	test triserial, finely perforate, margin distinctly segmented, longitudinal costae, same as *Uvigerina porrecta* Brady
Sphaeroidina bulloides d'Orbigny	RA, PCA, CA	test subglobular, finely perforate, small crescent-shaped aperture; considerable range in size
Uvigerina peregrina Cushman	RA, PCA, CA	test triserial, ovate, finely perforate, longitudinal costae sometimes hispid on final chambers; this species is variable in the number, thickness, and length of costae and spines (var. *hispidocostata* Cushman, var. *parvula* Cushman, var. *typica* Cushman)

[a]Indicated are taxa whose relative abundances (RA) are depicted in this paper, as well as taxa used in the principal components analyses (PCA) and cluster analyses (CA). Taxonomic descriptions and/or discussion are provided for select taxa.

ate margins where the timing and magnitude of sea level change and sediment flux are not always well constrained.

6. Conclusions

[39] Analysis of benthic foraminiferal populations in two well-dated piston cores from the slopes of Ashmore Trough provide insights into the paleoenvironmental history of this modern tropical mixed siliciclastic-carbonate system. In particular, over the past ~83 ka, benthic foraminiferal populations indicate three major assemblages, which appear to be linked to sea level-driven changes in the fluxes of siliciclastic, carbonate, and organic matter. The *Uvigerina peregrina-Bolivina robusta* assemblage is characterized by infaunal taxa indicative of increased carbon flux and/or decreased bottom water oxygen concentrations. This assemblage dominates during early regression (~83 to 70 ka), a time of greatly elevated siliciclastic and organic carbon flux into Ashmore Trough. In contrast, the *Globocassidulina subglobosa* assemblage is dominated by *Globocassidulina subglobosa*, a species associated with decreased carbon flux and/or increased bottom water oxygen concentrations. This assemblage dominates from late regression through early transgression (~70 to 11 ka), when siliciclastic and organic carbon fluxes to slopes of Ashmore Trough were at a minimum. The *Planorbulina mediterranensis* assemblage is characterized by epifaunal, attached or temporally attached taxa typical of neritic waters. This assemblage prevailed from late transgression to highstand (~11 ka to present), coincident with elevated fluxes of neritic carbonate, attributed to "highstand shedding", to the slopes of Ashmore Trough.

Appendix A

[40] Table A1 lists key benthic taxa that account for >2% of the assemblages in at least one sample. Indicated are taxa whose relative abundances are depicted in this paper, as well as taxa used in the principal components analyses and cluster analyses. Taxonomic descriptions and/or discussion are provided for select taxa.

References

Berger, W. H., and L. Diester-Haass (1988), Paleoproductivity: The benthic/planktonic ratio in foraminifera as a productivity index, *Mar. Geol.*, *81*, 15–25.

Bernhard, J., and E. Alve (1996), Survival, ATP pool, and ultrastuctural characterization of benthic foraminifera from Drammensfjord (Norway): Response to anoxia, *Mar. Micropaleontol.*, *28*, 5–17.

Bernhard, J., and B. K. SenGupta (1999), Foraminifera of oxygen-depleted environments, in *Modern Foraminifera*, edited by B. K. Sen Gupta, pp. 201–216, Kluwer Acad., Dordrecht, Netherlands.

Boltovskoy, E., and R. Wright (1976), *Recent Foraminifera*, 136 pp. Junk, Amsterdam.

Brunskill, G. J., K. J. Woolfe, and I. Zagorskis (1995), Distribution of riverine sediment chemistry on the shelf, slope and rise of the Gulf of Papua, *Geo Mar. Lett.*, *15*, 160–165.

Buzas, M. A., and T. G. Gibson (1969), Species diversity: Benthic foraminifera in the western North Atlantic, *Science*, *163*, 72–75.

Chappell, J. (2002), Sea level changes forced ice breakouts in the Last Glacial cycle: New results coral terraces, *Quat. Sci. Rev.*, *21*, 1229–1240.

Corliss, B. H., and C. Chen (1988), Morphotype patterns of Norwegian Sea deep-sea benthic foraminifera and ecological implications, *Geology*, *16*, 716–719.

Corliss, B. H., and E. Fois (1990), Morphotype analysis of deep-sea foraminifera from the Northwest gulf of Mexico, *Palaios*, *5*, 589–605.

Culver, S. J., and M. A. Buzas, (2000), Response of shallow water foraminiferal paleocommunities to global and regional environmental change, in *Biotic Response to Global Change: The Last 145 Million Years*, edited by S. J. Culver and P. F. Rawson, pp. 122–134, Cambridge Univ. Press, Cambridge, U. K.

Davis, J. C. (1986), *Statistics and Data Analysis in Geology*, John Wiley, Hoboken, N. J.

Diester-Haass, L. (1978), Sediments as indicators of upwelling, in *Upwelling Ecosystems*, edited by R. Boje and M. Tomczak, pp. 261–281, Springer, Berlin.

Droxler, A. W. (1984), Late Quaternary glacial cycles in the Bahamian deep basins and in the adjacent Atlantic Ocean, 120 pp., dissertation, Univ. of Miami, Coral Gables, Fla.

Droxler, A. W., and W. Schlager (1985), Glacial versus interglacial sedimentation rates and turbidite frequency in the Bahamas, *Geology*, *13*, 799–802.

Dunbar, G. B., G. R. Dickens, and R. M. Carter (2000), Sediment flux across the Great Barrier Reef shelf to the Queensland Trough over last 300 ky, *Sediment. Geol.*, *133*, 49–92.

Fairbanks, R. G., R. A. Mortlock, T. Chiu, L. Cao, A. Kaplan, T. Guilderson, T. W. Fairbanks, and A. L. Bloom (2005), Radiocarbon calibration curve spanning 0 to 50000 years BP based on paired ^{230}Th/^{234}U/^{238}U and ^{14}C dates on pristine corals, *Quat. Sci. Rev.*, *24*, 1781–1796.

Francis, J. M., B. Olson, G. R. Dickens, A. W. Droxler, L. Beaufort, T. De Garidel-Thoron, S. J. Bentley, L. C. Peterson, and B. Opdyke (2006), High siliciclastic flux during the last sea level transgression, Ashmore Trough, Gulf of Papua, paper presented at Annual Meeting, Am. Assoc. of Petrol. Geol., Houston, Tex.

Gibson, T. G. (1989), Planktonic:benthonic foraminiferal ratios: Modern patterns and Tertiary applicability, *Mar. Micropaleontol.*, *15*, 29–52.

Gooday, A. J. (1988), A response by benthic foraminifera to the deposition of phytodetritus in the deep sea, *Nature*, *332*, 70–73.

Gooday, A. J. (1993), Deep-sea benthic foraminiferal species which exploit phytodetritus: Characteristics features and controls on distribution, *Mar. Micropaleontol.*, 22, 187–205.

Handford, C. R., and R. G. Loucks (1993), Carbonate depositional sequences and systems tracts—Responses of carbonate platforms to relative sea-level changes, in *Carbonate Sequence Stratigraphy: Recent Developments and Applications*, edited by R. G. Loucks and J. F. Sarg, *AAPG Mem.*, 57, 3–41.

Harman, H. H. (1976), *Modern Factor Analysis*, Univ. of Chicago Press, Chicago, Ill.

Harris, P. T., E. K. Baker, A. R. Cole, and S. A. Short (1993), Preliminary study of sedimentation in the tidally dominated Fly River Delta, Gulf of Papua, *Cont. Shelf Res.*, 13, 441–472.

Harris, P. T., C. B. Pattiaratchi, J. B. Keene, R. W. Dalrymple, J. V. Gardner, E. K. Baker, A. R. Cole, D. Mitchell, P. Gibbs, and W. W. Schroeder (1996), Late Quaternary deltaic and carbonate sedimentation in the Gulf of Papua foreland basin: response to sea-level change, *J. Sediment. Res.*, 66, 801–819.

Harris, P. T., A. Heap, V. Passlow, M. Hughes, J. Daniell, M. Hemer, and O. Anderson (2005), Tidally incised valleys on tropical carbonate shelves: An example from the northern Great Barrier Reef, Australia, *Mar. Geol.*, 220, 181–204.

Herguera, J. C., and W. H. Berger (1991), Paleoproductivity from benthic foraminifera abundance: Glacial to postglacial change in the west equatorial Pacific, *Geology*, 19, 1173–1176.

Jorissen, F. J. (1999), Benthic foraminiferal microhabitats below the sediment-water interface, in *Modern Foraminifera*, pp. 161–179, Kluwer Acad., Dordrecht, Netherlands.

Jorissen, F. J., D. M. Barmawidjaja, S. Puskaric, and G. J. van der Zwaan (1992), Vertical distribution of benthic Foraminifera in the northern Adriatic Sea: The relation with high organic flux, *Mar. Micropaleontol.*, 26, 3–15.

Jorissen, F. J., H. C. De Stigter, and J. G. V. Widmark (1995), A conceptual model explaining benthic foraminiferal microhabitats, *Mar. Micropaleontol.*, 26, 3–15.

Jorry, S. J., A. W. Droxler, G. Mallarino, G. R. Dickens, S. J. Bentley, L. Beaufort, and L. C. Peterson (2008), Bundled turbidite deposition in the Central Pandora Trough (Gulf of Papua) since Last Glacial Maximum: Linking sediment and accumulation to sea level fluctuations at millennial timescale, *J. Geophys. Res.*, doi:10.1029/2006JF000649, in press.

Kaiho, K. (1994), Benthic foraminifera dissolved oxygen index and dissolved-oxygen levels in the modern ocean, *Geology*, 22, 719–722.

Kaiho, K. (1999), Effect of organic carbon flux and dissolved oxygen on the benthic foraminiferal oxygen index (BFOI), *Mar. Micropaleontol.*, 37, 67–76.

Lambeck, K., T. M. Esat, and E.-K. Potter (2002), Links between climate and sea levels for the past three million years, *Nature*, 419, 199–206.

Leckie, R. M., and H. C. Olson (2003), Foraminifera as proxies of sea-level change on siliciclastic margins, in *Micropaleontologic Proxies for Sea-Level Change and Stratigraphic Discontinuities*, edited by H. C. Olson and R. M. Leckie, *Spec. Publ. SEPM Soc. Sediment. Geol.*, 17, 5–19.

Linke, P., and G. F. Lutze (1993), Microhabitat preferences of benthic foraminifera—A static concept or a dynamic adaptation to optimize food acquisition?, *Mar. Micropaleontol.*, 20, 215–234.

Lisiecki, L. E., and M. E. Raymo (2005), A Pliocene-Pleistocene stack of 57 globally distributed benthic δ^{18}O records, *Paleoceanography*, 20, PA1003, doi:10.1029/2004PA001071.

Loeblich, A. R., and H. Tappan (1994), Foraminifera of the Sahul Shelf and Timor Sea, *Spec. Publ. Cushman Found. Foraminiferal Res.*, 31, 661 pp.

Lohmann, G. (1978), Abyssal benthonic foraminifera as hydrographic indicators in the western South Atlantic Ocean, *J. Foraminiferal Res.*, 8(1), 6–34.

Loubere, P. (1994), Quantitative estimation of surface ocean productivity and bottom water oxygen signals in deep water benthic foraminifera, *Paleoceanography*, 9, 723–737.

Loubere, P. (1996), The surface ocean productivity and bottom water oxygen signals in deep water benthic foraminiferal assemblages, *Mar. Micropaleontol.*, 28, 247–261.

Loubere, P. (1998), The impact of seasonality on the benthos as reflected in the assemblages of deep sea foraminifera, *Deep Sea Res., Part I*, 45, 409–432.

Loubere, P., and M. Fariduddin (1999), Benthic foraminifera and the flux of organic carbon to the seabed, in *Modern Foraminifera*, edited by B. K. Sen Gupta, pp. 181–199, Kluwer Acad., Dordrecht, Netherlands.

Loubere, P., G. Banonis, and R. Jakiel (1988), *Globocassidulina subglobosa* (Brady): Environmental control of species abundance and specimen test size, *J. Foraminiferal Res.*, 18(1), 6–15.

Mackensen, A., D. Futterer, H. Groe, and G. Schmiedl (1993), Benthic foraminiferal assemblages from the eastern South Atlantic Polar Front region between 35 and 57 S: Distribution, ecology and fossilization potential, *Mar. Micropaleontol.*, 22, 33–69.

Miller, K. G., and G. Lohmann (1982), Environmental distribution of recent benthic foraminifera in the northeast United States continental slope, *Geol. Soc. Am. Bull.*, 92, 200–206.

Milliman, J. D. (1995), Sediment discharge to the ocean from small mountainous rivers: The New Guinea example, *Geo Mar. Lett.*, 15, 127–133.

Muhammad, Z., S. J. Bentley, L. A. Febo, A. W. Droxler, G. R. Dickens, L. C. Peterson, and B. N. Opdyke (2008), Excess ^{210}Pb inventories and fluxes along the continental slope and basins of the Gulf of Papua, *J. Geophys. Res.*, doi:10.1029/2006JF000676, in press.

Murray, J. W. (1991), *Ecology and Palaeoecology of Benthic Foraminifera*, 397 pp., Longman Sci., Harlow, UK.

National Science Foundation (2003), *Margins Science Plans* 170 pp., Lamont-Doherty Earth Obs., Palisades, NY.

Page, M. K., G. R. Dickens, and G. B. Dunbar (2003), A downunder tropical view of Quaternary sequence stratigraphy: A siliciclastic accumulation on slopes east of the Great Barrier Reef since the Last Glacial Maximum, *Geology*, 31, 1013–1016.

Parker, W. C., and A. J. Arnold, (1999), Quantitative methods of data analysis in foraminiferal ecology, in *Modern Foraminifera*, edited by B. K. Sen Gupta, pp. 71–89, Kluwer Acad., Dordrecht, Netherlands.

Phleger, F. B. (1960), *Ecology and Distribution of Recent Foraminifera*, 297 pp., Johns Hopkins Press, Baltimore, Md.

Phleger, F. B., and F. L. Parker (1951), Ecology of foraminifera, northwest Gulf of Mexico, *Mem. Geol. Soc. Am.*, 46, 152 pp.

Pickard, G. L., J. R. Donguy, C. Henin, and R. Rougerie. (1977), *A Review of the Physical Oceanography of the Great Barrier Reef and Western Coral Sea, Monogr. Ser.*, vol. 2, 134 pp., Aust. Inst. of Mar. Sci., Cape Ferguson, Queensl., Australia.

Poag, C. W. (1981), *Ecologic Atlas of Benthic Foraminifera of the Gulf of Mexico*, 174 pp., Mar. Sci. Int., Woods Hole, Mass.

Rathburn, A. E., and B. H. Corliss (1994), The ecology of living (stained) deep-sea benthic foraminifera form the Sulu Sea, *Paleoceanography*, 9, 87–150.

Rosoff, D. B., and B. H. Corliss (1992), An analysis of recent deep-sea benthic foraminiferal morphotypes from the Norwegian and Greenland seas, *Palaeoceanogr. Palaeoclimatol. Palaeoecol.*, 91, 13–20.

Schlager, W., J. J. G. Reijmer, and A. W. Droxler (1994), Highstand shedding of carbonate platforms, *J. Sediment. Res.*, 64, 270–281.

Schmiedl, G., A. Mackensen, and P. Muller (1997), Recent benthic foraminifera from the eastern South Atlantic Ocean: Dependence on food supply and water masses, *Mar. Micropaleontol.*, 32, 249–288.

Sen Gupta, B. K. (1999a), *Modern Foraminifera*, Kluwer Acad., Dordrecht, Netherlands.

Sen Gupta, B. K. (1999b), Foraminifera in marginal marine environments, in *Modern Foraminifera*, edited by B. K. Sen Gupta, pp. 141–159, Kluwer Acad., Dordrecht, Netherlands.

Stuiver, M., and P. J. Reimer (1993), Extended ^{14}C database and revised CALIB radiocarbon calibration program, *Radiocarbon*, 35, 215–230.

Thomas, E., and A. J. Gooday (1996), Cenozoic deep-sea benthic foraminifers: Tracers for changes in oceanic productivity?, *Geology*, 24, 355–358.

Walsh, J. P., and C. A. Nittrouer (2003), Contrasting styles of off-shelf sediment accumulation in New Guinea, *Mar. Geol.*, 196, 105–125.

Wolanski, E., and D. M. Alongi (1995), A hypothesis for the formation of a mud bank in the Gulf of Papua, *Geo Mar. Lett.*, 15, 166–171.

Wolanski, E., A. Norro, and B. King (1995), Water circulation in the Gulf of Papua, *Cont. Shelf Res.*, 15, 185–212.

Wyrtki, K. (1960), Surface circulation in the Coral and Tasman Seas, *Tech. Pap. 8*, CSIRO Aust. Div. of Fish. and Oceanogr., Cronulla, N.S.W., Australia.

Wyrtki, K. (1962), The subsurface water masses in the western South Pacific Ocean, *Aust. J. Freshwater Res.*, 13, 18–47.

————————

S. J. Bentley, Earth Sciences Department, Memorial University of Newfoundland, St. John's, NL, Canada A1B 3X5.

B. E. Carson and J. M. Francis, Chevron Energy Technology Company, 1500 Louisiana, Houston, TX 77002, USA. (brookecarson@chevron.com)

G. R. Dickens and A. W. Droxler, Department of Earth Science, Rice University, Houston, TX 77005, USA.

S. J. Jorry, Division Etudes and Conseils, Beicip-Franlab, 232 Avenue Napoleon Bonaparte, F-92500, Rueil-Malmaison, France.

R. M. Leckie, Department of Geosciences, University of Massachusetts, Amherst, MA 01003, USA.

B. N. Opdyke, Department of Earth and Marine Science, Australian National University, Canberra, ACT 0200, Australia.

L. C. Peterson, Rosenstiel School of Marine and Atmospheric Science, University of Miami, Miami, FL 33149, USA.